

## PDF hosted at the Radboud Repository of the Radboud University Nijmegen

The following full text is a publisher's version.

For additional information about this publication click this link.

<http://hdl.handle.net/2066/16382>

Please be advised that this information was generated on 2022-08-25 and may be subject to change.

# Synthesis and Supramolecular Chemistry of Novel Liquid Crystalline Crown Ether-Substituted Phthalocyanines: Toward Molecular Wires and Molecular Ionoelectronics

Cornelus F. van Nostrum,<sup>†</sup> Stephen J. Picken,<sup>‡</sup> Arend-Jan Schouten,<sup>§</sup> and Roeland J. M. Nolte<sup>\*,†</sup>

Contribution from the Department of Organic Chemistry, N.S.R. Center, University of Nijmegen, Toernooiveld, 6525 ED Nijmegen, The Netherlands, Akzo Nobel Central Research, Physical Chemistry Department, P.O. Box 9300, 6800 SB Arnhem, The Netherlands, and Laboratory of Polymer Science, University of Groningen, Nijenborgh 4, 9747 AG Groningen, The Netherlands

Received March 2, 1995<sup>⊗</sup>

**Abstract:** The synthesis of the metal-free and the dihydroxysilicon derivatives of tetrakis[4',5'-bis(decoxy)benzo-18-crown-6]phthalocyanine is described. The metal-free phthalocyanine is liquid crystalline and exhibits a crystalline phase to mesophase transition at 148 °C. The structures of the crystalline phase and the mesophase are determined by X-ray measurements. The metal-free compound strongly aggregates in chloroform solution to form a gel. Electron micrographs show that this gel contains a network of fibers, each of which is built up of parallel strands of supermolecules having the thickness of one molecule and a length of several micrometers. The strands are formed by a process of self-assembly involving up to 10<sup>4</sup> molecules. They can be considered as being molecular cables, containing a central electron wire, four ion channels, and a surrounding insulating hydrocarbon mantle. The silicon derivative contains two axial hydroxy groups which prevent the molecule from aggregating. This compound is not liquid crystalline. It forms a stable monolayer at the air–water interface. In this layer, the phthalocyanine planes are oriented parallel to the water surface. The monolayers can be transferred onto glass substrates by a Y-type deposition. The resulting Langmuir–Blodgett film is built up of bilayers containing slipped face-to-face phthalocyanine dimers. The monolayer is capable of binding alkali metal ions from the subphase, as is concluded from surface area–surface pressure isotherms. The binding constant for potassium ions has been determined by analyzing the isotherms as a function of the concentration of this metal ion. The dihydroxysilicon phthalocyanine can be polymerized to form a polysiloxane.

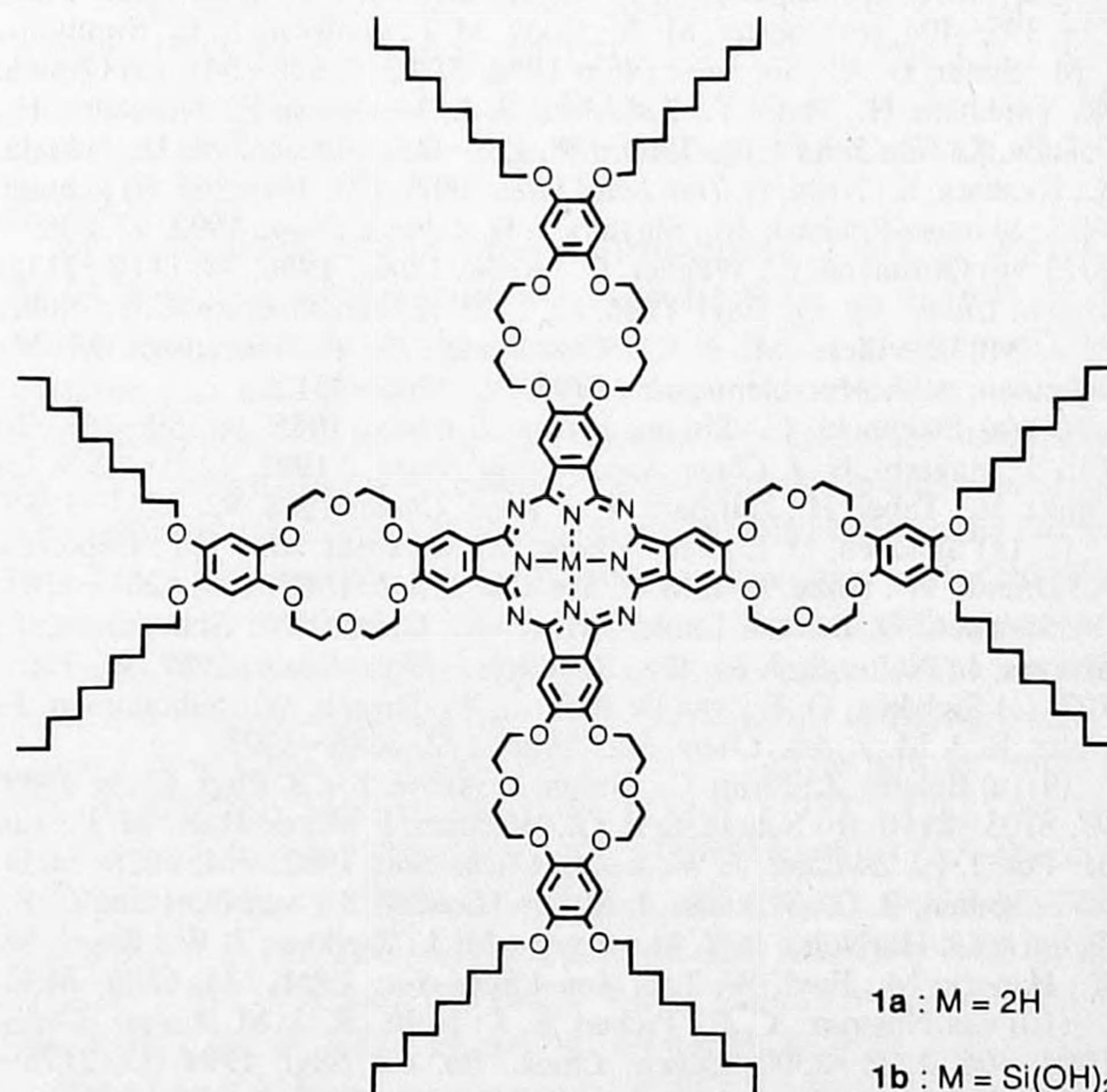
## Introduction

The study of nanometer-sized structures and molecular materials, which are formed by self-organization, is of great interest for the construction of devices that are small and fast and that can store information with high density.<sup>1</sup> Molecular electronics and molecular ionics are new scientific fields dealing with this subject.<sup>2,3</sup> In the latter case, the information storage and processing are achieved with the help of ions. An important step in this process is the nonlinear complexation of ions, which allows for reliable switching between on and off states.<sup>3d</sup> Furthermore, the construction of supramolecular wires and channels capable of transporting electrons and ions is a great challenge.<sup>4</sup>

Phthalocyanines (Pcs) belong to a class of compounds that has potential for application in functional nanostructures. Phthalocyanines substituted with long, flexible hydrocarbon chains can self-assemble to form columnar mesophases,<sup>5</sup> Langmuir–Blodgett (LB) multilayers,<sup>5e,6</sup> or aggregates in solution.<sup>6f,7</sup>

Recently, we showed that crown ether-substituted Pcs can be stacked to create ion conducting channels.<sup>8</sup> The electron conducting properties of these structures have been extensively studied.<sup>5d,8b,9</sup>

In this paper we describe the synthesis and self-organizing properties of the metal-free and silicon Pcs **1a,b**.<sup>10</sup> These compounds contain a central Pc core, four 18-crown-6 rings, and a total of eight decoxy chains linked via benzene units to the crown ether rings. They were designed to develop systems



<sup>†</sup> University of Nijmegen.

<sup>‡</sup> Akzo Nobel Central Research, Arnhem.

<sup>§</sup> University of Groningen.

<sup>⊗</sup> Abstract published in *Advance ACS Abstracts*, September 1, 1995.

(1) Whitesides, G. M.; Mathias, J. P.; Seto, C. T. *Science* **1991**, *254*, 1312–1319.

(2) Lehn, J.-M. *Angew. Chem.* **1988**, *100*, 91–116; *Angew. Chem., Int. Ed. Engl.* **1988**, *27*, 89.

(3) (a) Lehn, J.-M. *Angew. Chem.* **1990**, *102*, 1347–1362; *Angew. Chem., Int. Ed. Engl.* **1990**, *29*, 1304. (b) Metzger, R. M.; Panetta, C. A. *New J. Chem.* **1991**, *15*, 209–221. (c) Simon, J.; Sirlin, C. *Pure Appl. Chem.* **1989**, *61*, 1625–1629. (d) Simon, J.; Engel M. K.; Soulié, C. *New J. Chem.* **1992**, *16*, 287–293.

(4) (a) Harada, A.; Li, J.; Kamachi, M. *Nature* **1993**, *364*, 516–518. (b) Khazanovich, N.; Granja, J. R.; McRee, D. E.; Milligan, R. A.; Ghadiri, M. R. *J. Am. Chem. Soc.* **1994**, *116*, 6011–6012.

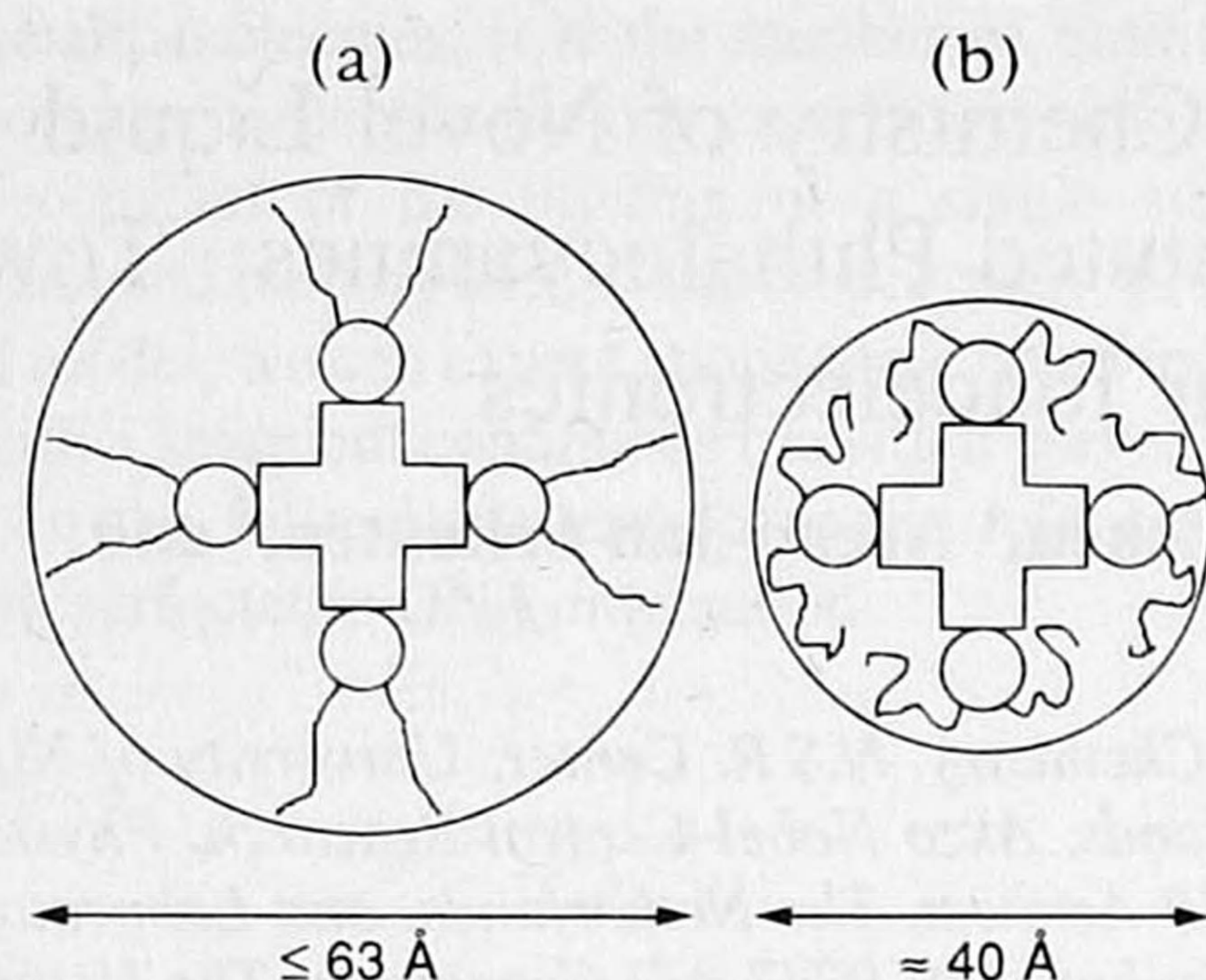


**Figure 1.** Schematic representation of the disk-like molecules **1** showing the two limiting diameters  $L$ , as estimated from CPK molecular models: (a) fully elongated decoxy chains (b) decoxy chains bending back.

that combine the properties of electron conduction, ion conduction, and liquid crystallinity. CPK molecular models show that molecules **1a,b** display a high degree of shape anisotropy, which is favorable for the formation of a (columnar) mesophase. Taking as the thickness of the molecules a value of  $4.2 \text{ \AA}$ ,<sup>8b,11</sup> the length over thickness ( $L/d$ ) aspect ratio is in the range of 9.5–15, depending on the conformation of the peripheral decoxy chains (see Figure 1). We will show in this paper that **1a** indeed forms a thermotropic mesophase. Moreover, this compound self-assembles in chloroform solution to yield an extremely long supramolecular cable. Phthalocyanine **1b** forms stable monolayers at the air–water interface. These monolayers can bind alkali metal ions from the subphase and can be transferred onto solid substrates, giving a LB film. Preliminary results indicate that **1b** can be polymerized to form an axial polysiloxane.

## Experimental Section

**Materials and Methods.** All solvents were dried before use. Merck Kieselgel 60H was used for chromatography. 3,4-Dihydroxybenzaldehyde was recrystallized twice from *o*-xylene.  $\text{K}_2\text{CO}_3$  was dried in an oven before use. Potassium nitrosodisulfonate (Fremy's radical) was prepared according to the method of Zimmer *et al.*<sup>12</sup> Catechol was recrystallized from toluene. The tetrahydropyranyl ether of 2-(2'-chloroethoxy)ethanol was synthesized according to the procedure of Kyba *et al.*<sup>13</sup> *p*-Toluenesulfonyl chloride was recrystallized from hexane. (*N,N*-Dimethylamino)ethanol and  $\text{SiCl}_4$  were freshly distilled before use. Quinoline was freshly distilled from barium oxide. All other reagents were used as supplied, without further purification.

Melting points were determined with a Reichert hot-stage microscope and are uncorrected. Infrared (IR) spectra were recorded with a Perkin Elmer 28 infrared spectrophotometer or a Perkin Elmer 1720-X infrared Fourier transform spectrophotometer. UV/vis spectra were obtained with a Perkin Elmer Lambda 5 spectrophotometer.  $^1\text{H}$  NMR spectra were obtained with Varian EM 390, Bruker AC-100, or Bruker WM-400 instruments. Chemical shifts are reported in ppm downfield from internal TMS standard. Abbreviations used are as follows: s, singlet; d, doublet; t, triplet; m, multiplet; br, broad. Electronic ionization (EI), chemical ionization (CI), and fast atom bombardment (FAB) mass spectra (MS) were obtained with a VG-7070E apparatus. Elemental analysis were carried out on an EA 1108 Carlo Erba instrument.

Differential scanning calorimetry (DSC) data were obtained with a Mettler DSC 12E instrument. The measurements were carried out under an inert atmosphere with heating and cooling rates of  $10 \text{ }^\circ\text{C}\cdot\text{min}^{-1}$ . Thermogravimetric analysis (TGA) was carried out on a Perkin Elmer System 4 under inert atmosphere. For polarization microscopy, a Leitz Orthoplan polarization microscope was used, equipped with a Mettler FP80/FP82 hot stage. Small-angle X-ray scattering (SAXS) curves were recorded using a Siemens D5000 reflection diffractometer with a HTK oven and a  $\text{Cu K}\alpha$  source with a wavelength of  $1.5406 \text{ \AA}$ .

Transmission electron microscopy was carried out with a Philips TEM 201 instrument. Small drops of the samples were placed on carbon-coated grids, the material was allowed to adsorb for 1 min, and then the grids were blotted dry by touching the edges with filter paper. Finally, the structures were visualized by shadowing with platinum at an angle of  $\sim 45^\circ$ .

Monolayers at the air–water interface were studied by measuring pressure–area isotherms on a computer-controlled Lauda film balance (FW 2) and on a home-built film balance, in both cases using water that was purified by a Milli-Q filtration system as the subphase. A sample was dissolved in chloroform (spectroscopic quality,  $\sim 1 \text{ mg}\cdot\text{mL}^{-1}$ ) and spread on the water surface, and isotherms were recorded at a compression speed of  $\sim 30 \text{ \AA}^2\cdot\text{molecule}^{-1}\cdot\text{min}^{-1}$  at  $20 \text{ }^\circ\text{C}$ . The water surface was visualized during compression with a Brewster angle microscope (NFT BAM-1) equipped with a 10 mW He–Ne laser with a beam diameter of 0.68 mm operating at 632.8 nm. Reflections were detected using a CCD camera. Glass substrates were cleaned ultrasonically with chloroform, treated with concentrated sulfochromic acid at  $80 \text{ }^\circ\text{C}$  for 2 h, washed several times with Milli-Q water, cleaned again ultrasonically in acetone and in chloroform, and finally stored in methanol. Before use, the substrate was rinsed with chloroform, partially hydrophobized by treatment with a boiling mixture of chloroform and hexamethyldisilazane, and finally rinsed with chloroform. Deposition was carried out by vertically dipping the substrate with a speed of  $10 \text{ mm}\cdot\text{min}^{-1}$  through the monolayer, which was equilibrated for 1.5 h at constant surface pressure and temperature. UV/vis spectroscopy on the resulting film was carried out with an SLM-Aminco 3000 diode array spectrophotometer.

**Syntheses. 3,4-Bis(decoxy)benzaldehyde (3).** 3,4-Dihydroxybenzaldehyde (10.6 g, 0.077 mol) and 1-bromodecane (35.6 g, 0.161 mol) were dissolved in DMF (100 mL). Nitrogen gas was bubbled through the solution for 10 min.  $\text{K}_2\text{CO}_3$  (23.8 g, 0.172 mol) was then added,

(11) Sirlin, C.; Bosio, L.; Simon, J.; Ahsen, V.; Yilmazer, E.; Bekaroglu, Ö. *Chem. Phys. Lett.* **1987**, *139*, 362–364.

(12) Zimmer, H.; Lankin, D. C.; Horgan, S. W. *Chem. Rev.* **1971**, *71*, 229–246.

(13) Kyba, E. P.; Helgeson, R. C.; Madan, K.; Gokel, G. W.; Tarnowski, T. L.; Moore, S. S.; Cram, D. J. *J. Am. Chem. Soc.* **1977**, *99*, 2564–2571.

(5) (a) Piechocki, C.; Simon, J.; Skoulios, A.; Guillon, D.; Weber, P. *J. Am. Chem. Soc.* **1982**, *104*, 5245–5247. (b) Engel, M. K.; Bassoul, P.; Bosio, L.; Lehmann, H.; Hanack, M.; Simon, J. *Liq. Cryst.* **1993**, *15*, 709. (c) Cho, I.; Lim, Y. *Mol. Cryst. Liq. Cryst.* **1988**, *154*, 9–26. (d) van der Pol, J. F.; Neeleman, E.; Zwikker, J. W.; Nolte, R. J. M.; Drenth, W.; Aerts, J.; Visser, R.; Picken, S. J. *Liq. Cryst.* **1989**, *6*, 577–592. (e) van Nostrum, C. F.; Bosman, A. W.; Gelinck, G. H.; Schouten, P. G.; Warman, J. M.; Kentgens, A. P. M.; Meijerink, A.; Picken, S. J.; Devillers, M. A. C.; Sohling, U.; Schouten, A.-J.; Nolte, R. J. M. *Chem. Eur. J.* **1995**, *1*, 171–182.

(6) (a) Barger, W. R.; Snow, A. W.; Wohltjen, H.; Jarvis, N. L. *Thin Solid Films* **1985**, *133*, 197–206. (b) Cook, M. J.; Dunn, A. J.; Daniel, M. F.; Hart, R. C. O.; Richardson, R. M.; Roser, S. J. *Thin Solid Films* **1988**, *159*, 395–404. (c) Chester, M. A.; Cook, M. J.; Gallivan, S. L.; Simmons, J. M.; Slater, D. A. *Thin Solid Films* **1992**, *210/211*, 538–541. (d) Ogawa, K.; Yonehara, H.; Shoji, T.; Kinoshita, S.-I.; Maekawa, E.; Nakahara, H.; Fukuda, K. *Thin Solid Films* **1989**, *178*, 439–443. (e) Nakahara, H.; Fukuda, K.; Kitahara, K.; Nishi, H. *Thin Solid Films* **1989**, *178*, 361–366. (f) Schutte, W. J.; Sluyters-Rehbach, M.; Sluyters, J. H. *J. Phys. Chem.* **1993**, *97*, 6069–6073. (g) Orthmann, E.; Wegner, G. *Angew. Chem.* **1986**, *98*, 1114–1115; *Angew. Chem., Int. Ed. Engl.* **1986**, *25*, 1105. (h) van Nostrum, C. F.; Nolte, R. J. M.; Devillers, M. A. C.; Oostergetel, G. T.; Teerenstra, M. N.; Schouten, A.-J. *Macromolecules* **1993**, *26*, 3306–3312.

(7) (a) Piechocki, C.; Simon, J. *New J. Chem.* **1985**, *9*, 159–163. (b) Tai, S.; Hayashi, N. *J. Chem. Soc., Perkin Trans. 2* **1991**, 1275–1279. (c) Fujiki, M.; Tabei, H.; Kurihara, T. *J. Phys. Chem.* **1988**, *92*, 1281–1285.

(8) (a) Sielcken, O. E.; van Tilborg, M. M.; Roks, M. F. M.; Hendriks, R.; Drenth, W.; Nolte, R. J. M. *J. Am. Chem. Soc.* **1987**, *109*, 4261–4265. (b) Sielcken, O. E.; van Lindert, H. C. A.; Drenth, W.; Schoonman, J.; Schram, J.; Nolte, R. J. M. *Ber. Bunsenges. Phys. Chem.* **1989**, *93*, 702–707. (c) Sielcken, O. E.; van de Kuil, L. A.; Drenth, W.; Schoonman, J.; Nolte, R. J. M. *J. Am. Chem. Soc.* **1990**, *112*, 3086–3093.

(9) (a) Belarbi, Z.; Sirlin, C.; Simon, J.; André, J.-J. *J. Phys. Chem.* **1989**, *93*, 8105–8110. (b) Schouten, P. G.; Warman, J. M.; de Haas, M. P.; van der Pol, J. F.; Zwikker, J. W. *J. Am. Chem. Soc.* **1992**, *114*, 9028–9034. (c) Schouten, P. G.; Warman, J. M.; de Haas, M. P.; van Nostrum, C. F.; Gelinck, G. H.; Nolte, R. J. M.; Copyn, M. J.; Zwikker, J. W.; Engel, M. K.; Hanack, M.; Ford, W. T. *J. Am. Chem. Soc.* **1994**, *116*, 6880–6894.

(10) van Nostrum, C. F.; Picken, S. J.; Nolte, R. J. M. *Angew. Chem.* **1994**, *106*, 2298–2300; *Angew. Chem., Int. Ed. Engl.* **1994**, *33*, 2173–2175.

and the mixture was stirred at 100 °C under a nitrogen atmosphere for 16 h. After cooling, water (200 mL) was added, and the product was extracted with chloroform (4 × 50 mL). The combined extracts were washed with water (40 mL), dried over MgSO<sub>4</sub>, and filtered, and the solvent was evaporated under high vacuum. The resulting solid was recrystallized from acetone at 4 °C. Yield: 27.1 g (84%). White solid, mp 64 °C. IR (KBr): 810, 865 (Ar-H), 1230, 1270 (Ar-O-C), 1505, 1585 (Ar), 1685, 2750 (H-C=O) cm<sup>-1</sup>. <sup>1</sup>H NMR (CDCl<sub>3</sub>, 90 MHz): δ 0.88 (t, 6H, CH<sub>3</sub>), 1.0–2.0 (m, 32H, CH<sub>2</sub>), 4.0 (t, 4H, CH<sub>2</sub>O), 6.88–7.52 (m, 3H, ArH), 9.85 (s, 1H, HC=O). MS (EI): *m/z* 418 (M<sup>+</sup>). Anal. Calcd for C<sub>27</sub>H<sub>46</sub>O<sub>3</sub>: C, 77.46; H, 11.07. Found: C, 77.42; H, 11.18.

**3,4-Bis(decoxy)phenol (4).** Benzaldehyde derivative **3** (31 g, 0.074 mol) was dissolved in chloroform (100 mL). Methanol (100 mL), 35% H<sub>2</sub>O<sub>2</sub> (9.5 g, 0.098 mol), and concentrated H<sub>2</sub>SO<sub>4</sub> (1 mL) were added, and the mixture was stirred at room temperature for 5 h. Water was added until two phases separated. The aqueous fraction was extracted with chloroform (2 × 25 mL). The combined organic solutions were washed with water (50 mL), dried over MgSO<sub>4</sub>, filtered, and rotary evaporated. The product was recrystallized from petroleum ether 40/60. Yield: 19.6 g (65%). Slightly brown solid, mp 78 °C. IR (KBr): 800, 825 (Ar-H), 1225, 1280 (Ar-O-C), 1510, 1605 (Ar), 3300 (OH) cm<sup>-1</sup>. <sup>1</sup>H NMR (CDCl<sub>3</sub>, 90 MHz): δ 0.88 (t, 6H, CH<sub>3</sub>), 1.0–1.9 (m, 32H, CH<sub>2</sub>), 3.9 (t, 4H, CH<sub>2</sub>O), 4.67 (br s, 1H, OH), 6.22–6.85 (m, 3H, ArH). MS (EI): *m/z* 406 (M<sup>+</sup>). Anal. Calcd for C<sub>26</sub>H<sub>46</sub>O<sub>3</sub>: C, 76.80; H, 11.40. Found: C, 76.60; H, 11.38.

**4,5-Bis(decoxy)-1,2-benzoquinone (5).** The following solutions were prepared: tetrabutylammonium chloride (2 g, 7 mmol) in water (370 mL), KH<sub>2</sub>PO<sub>4</sub> (1.5 g, 11 mmol) in water (100 mL), and phenol derivative **4** (7.5 g, 18 mmol) in THF (1250 mL). Potassium nitrosodisulfonate (10 g, 44 mmol) and the KH<sub>2</sub>PO<sub>4</sub> solution were quickly added to the stirred solution of Bu<sub>4</sub>NCl. The resulting mixture was added immediately, with vigorous stirring, to the solution of **4** in THF. After being stirred for 2 h at room temperature, the solution was saturated with NaCl and stirred for another 1 h while the solution was kept saturated with NaCl. The organic layer was separated, the THF evaporated under vacuum, and chloroform added to the resulting paste. The chloroform solution was washed with water, dried over MgSO<sub>4</sub>, filtered, and evaporated under vacuum. The product was recrystallized from acetone at 4 °C. Yield: 6.0 g (80%). Orange solid, mp 128 °C. IR (KBr): 850 (C=C-H), 1590 (C=C), 1665 (C=O), 2800–3000 (CH<sub>2</sub>/CH<sub>3</sub>), 3060 (C=C-H) cm<sup>-1</sup>. <sup>1</sup>H NMR (CDCl<sub>3</sub>, 90 MHz): δ 0.95 (t, 6H, CH<sub>3</sub>), 1.2–2.1 (m, 32H, CH<sub>2</sub>), 4.00 (t, 4H, CH<sub>2</sub>O), 5.75 (s, 2H, C=CH). MS (CI): *m/z* 422 (M<sup>+</sup>). Anal. Calcd for C<sub>26</sub>H<sub>44</sub>O<sub>4</sub>: C, 74.24; H, 10.54. Found: C, 73.87; H, 10.75.

**1,2-Bis(decoxy)-4,5-bis(acetoxy)benzene (6).** Powdered zinc (5 g, 76 mmol) was added with stirring to a refluxing mixture of benzoquinone derivative **5** (8.4 g, 20 mmol), concentrated acetic acid (35 mL), and acetic anhydride (35 mL). This mixture was subsequently refluxed for 30 min. The product crystallized on cooling. The solvent was removed under vacuum, and the resulting solid was dissolved in chloroform. This solution was filtered and concentrated under vacuum. The resulting product was recrystallized from acetone at 0 °C. Yield: 8.9 g (88%). White solid, mp 89 °C. IR (KBr): 1180, 1230 (Ar-O-C), 1510, 1605 (Ar), 1760 (C=O), 2800–3000 (CH<sub>2</sub>/CH<sub>3</sub>) cm<sup>-1</sup>. <sup>1</sup>H NMR (CDCl<sub>3</sub>, 100 MHz): δ 0.88 (t, 6H, CH<sub>3</sub>), 1.2–1.9 (m, 32H, CH<sub>2</sub>), 2.26 (s, 6H, CH<sub>3</sub>C=O), 3.94 (t, 4H, CH<sub>2</sub>O), 6.68 (s, 2H, ArH). MS (CI): *m/z* 506 (M<sup>+</sup>). Anal. Calcd for C<sub>30</sub>H<sub>50</sub>O<sub>6</sub>: C, 71.11; H, 9.95. Found: C, 71.42; H, 9.82.

**4,5-Dibromocatechol (8).** Catechol (38.8 g, 0.35 mol) was suspended in tetrachloromethane (400 mL) and cooled on ice. Molecular bromine (56 g, 0.70 mol), dissolved in tetrachloromethane (50 mL), was slowly added from a dropping funnel with stirring. Escaping HBr gas was caught in aqueous NaOH solution. After complete addition, the reaction mixture was stirred for 16 h at room temperature. The solid was filtered, washed with tetrachloromethane, dried, and stored under a nitrogen atmosphere. Yield: 86.3 g (91%). White solid, mp 119 °C. IR (KBr): 651 (ArBr), 1268 (ArO), 3443 (OH) cm<sup>-1</sup>. <sup>1</sup>H NMR (CDCl<sub>3</sub>, 90 MHz): δ 5.30 (s, 2H, OH), 7.06 (s, 2H, ArH).

**1,2-Bis[2'-(2''-hydroxyethoxy)ethoxy]-4,5-dibromobenzene (9).** Dibromocatechol (**8**) (134 g, 0.5 mol) was added to 1-butanol (1400 mL), and nitrogen gas was bubbled through this mixture for 10 min.

NaOH (40 g, 1 mol) was then added and dissolved by stirring and refluxing under a nitrogen atmosphere. The tetrahydropyranyl ether of 2-(2'-chloroethoxy)ethanol (208 g, 1 mol) was added dropwise to this solution with stirring. The reaction mixture was refluxed under nitrogen for 16 h. After the mixture was cooled, concentrated HCl (28 mL) was added, and the mixture was stirred for 1 h at room temperature. NaHCO<sub>3</sub> (140 g, 1.67 mol) was added, the mixture filtered, and the residue extracted with dichloromethane. The combined organic solutions were washed with 1 M aqueous NaOH and with water, dried over MgSO<sub>4</sub>, filtered, and concentrated under vacuum. The resulting liquid was distilled under vacuum. Yield: 109 g (49%). Clear, viscous oil, which slowly solidifies in the refrigerator, bp 240 °C (0.4 mmHg). IR (CHCl<sub>3</sub>): 650 (ArBr), 1050, 1120 (C-O-C), 1190, 1240 (Ar-O-C), 2800–3000 (CH<sub>2</sub>/CH<sub>3</sub>), 3200–3600 (OH) cm<sup>-1</sup>. <sup>1</sup>H NMR (CDCl<sub>3</sub>, 100 MHz): δ 3.47 (s, 2H, OH), 3.6–4.2 (m, 16H, CH<sub>2</sub>), 7.09 (s, 2H, ArH). MS (CI): *m/z* 444 (M<sup>+</sup>).

**1,2-Bis[2'-(2''-(*p*-toluenesulfonyloxy)ethoxy)ethoxy]-4,5-dibromobenzene (10).** A solution of compound **9** (68.4 g, 0.154 mol) in pyridine (125 mL) was cooled to -10 °C, and a solution of *p*-toluenesulfonyl chloride (70 g, 0.367 mol) in pyridine (125 mL) was added dropwise with stirring. This mixture was stirred for 2 h at -5 °C and then for one night at 0 °C. The reaction mixture was poured over ice (400 g), acidified with 6 M aqueous HCl, and extracted with dichloromethane (2 × 250 mL). The combined extracts were washed with water (2 × 250 mL), dried over MgSO<sub>4</sub>, filtered, and concentrated under vacuum. Yield: 108 g (93%) of a very viscous oil. The product was chromatographed on silica gel using 1:1 (v/v) ethyl acetate-hexane as the eluent, in portions that were sufficient for the next reaction step. A small amount was recrystallized from CDCl<sub>3</sub> to afford white needles, mp 87 °C. IR (CHCl<sub>3</sub>): 655 (ArBr), 1135 (C-O-C), 1170, 1350 (SO<sub>3</sub>), 1190, 1245 (Ar-O-C), 1595 (Ar) cm<sup>-1</sup>. <sup>1</sup>H NMR (CDCl<sub>3</sub>, 90 MHz): δ 2.38 (s, 6H, CH<sub>3</sub>), 3.6–4.25 (m, 16H, CH<sub>2</sub>), 7.03 (s, 2H, ArH), 7.25 (d, 4H, ArH), 7.73 (d, 4H, ArH). MS (FAB): *m/z* 752 (M<sup>+</sup>).

**{4',5'-Bis(decoxy)-4'',5''-dibromo}dibenzo[1',2'-b:1'',2''-k]-1,4,7,10,13,16-hexaoxacyclooctadeca-2,11-diene (11).** Compound **6** (9 g, 18 mmol) was suspended in 1-butanol (75 mL), and nitrogen gas was bubbled through the suspension for 10 min. Subsequently, NaOH (2.9 g, 72 mmol) was added and dissolved by stirring and refluxing under a nitrogen atmosphere. Compound **10** (13.5 g, 18 mmol) was added dropwise to the vigorously stirred solution (the addition can be facilitated by warming the viscous ditosylate **10** with a heat gun). The reaction mixture was refluxed with vigorous stirring under nitrogen for 16 h. After the reaction was complete, the mixture was acidified with concentrated HCl, and the solvent was removed by evaporation under reduced pressure. The resulting solid was dissolved in chloroform, and the solution was washed with water (3×), dried over MgSO<sub>4</sub>, and concentrated. The product was recrystallized from acetone (~750 mL). Yield: 8.7 g (58%). White powder, mp 129 °C. <sup>1</sup>H NMR (CDCl<sub>3</sub>, 100 MHz): δ 0.88 (t, 6H, CH<sub>3</sub>), 1.2–1.9 (m, 32H, CH<sub>2</sub>), 3.8–4.2 (m, 20H, CH<sub>2</sub>O), 6.57 (s, 2H, ROArH), 7.05 (s, 2H, BrArH). MS (CI): *m/z* 830 (M<sup>+</sup>). Anal. Calcd for C<sub>40</sub>H<sub>62</sub>Br<sub>2</sub>O<sub>8</sub>: C, 57.83; H, 7.52. Found C, 57.21; H, 7.59.

**{4',5'-Bis(decoxy)-4'',5''-dicyano}dibenzo[1',2'-b:1'',2''-k]-1,4,7,10,13,16-hexaoxacyclooctadeca-2,11-diene (12).** A mixture of dibromocrown ether **11** (8.3 g, 10 mmol), CuCN (2.7 g, 30 mmol), and pyridine (0.5 mL) in DMF (100 mL) was refluxed under a nitrogen atmosphere for ~40 h. After the reaction was complete (as checked by TLC), the mixture was cooled to room temperature and poured into 25% aqueous ammonia (200 mL). Air was bubbled through the mixture for 2 h. Subsequently, the reaction mixture was extracted with chloroform (4 × 50 mL). The extracts were washed with water (4 × 100 mL), dried over MgSO<sub>4</sub>, filtered, and concentrated. The resulting solid was chromatographed (silica gel, chloroform) and finally recrystallized from ethanol. Yield: 5.4 g (75%). White powder, mp 135 °C. IR (CHCl<sub>3</sub>): 869 (Ar-H), 1055, 1139 (C-O-C), 1288 (Ar-O-C), 1517, 1592 (Ar), 2233 (CN), 2856, 2928 (CH<sub>2</sub>), 3013 (Ar-H) cm<sup>-1</sup>. <sup>1</sup>H NMR (CDCl<sub>3</sub>, 100 MHz): δ 0.88 (t, 6H, CH<sub>3</sub>), 1.1–1.9 (m, 32H, CH<sub>2</sub>), 3.8–4.3 (m, 20H, CH<sub>2</sub>O), 6.56 (s, 2H, ROArH), 7.11 (s, 2H, NCArH). MS (CI): *m/z* 722 (M<sup>+</sup>). Anal. Calcd for C<sub>42</sub>H<sub>62</sub>N<sub>2</sub>O<sub>8</sub>: C, 69.78; H, 8.64; N, 3.87. Found: C, 69.45; H, 8.70; N, 3.71.

**Tetrakis{4',5'-bis(decoxy)benzo[1',2'-k]-1,4,7,10,13,16-hexaoxacy-**

**clooctadeca-2,11-dieno}[2,3-*b*:2',3'-*i*:2'',3''-*p*:2''',3'''-*w*]phthalocyanine (**1a**). A mixture of dicyanocrown ether **12** (0.75 g, 1.03 mmol) and (*N,N*-dimethylamino)ethanol (1 mL) was stirred and refluxed under a nitrogen atmosphere for 40 h. After cooling, chloroform (5 mL) was added, and the mixture was stirred for 3 h and then allowed to stand without stirring for 1 h. The precipitate was filtered off and recrystallized three times from chloroform. Yield: 0.245 g (30%). Dark green solid, K → M 148 °C. IR (CHCl<sub>3</sub>): 863 (Ar-H), 909, 954 (Pc), 1022 (N-H), 1101 (Pc), 1134 (C-O-C), 1280 (Ar-O-C), 1529, 1603 (Ar/Pc), 2853, 2925 (CH<sub>2</sub>), 3294 (N-H) cm<sup>-1</sup>. <sup>1</sup>H NMR (CDCl<sub>3</sub>, 400 MHz, 53 °C): δ 0.89 (br s, 24H, CH<sub>3</sub>), 1.2–1.8 (m, 128H, CH<sub>2</sub>), 3.6–4.9 (m, 80H, CH<sub>2</sub>O), 6.64 (s, 8H, ArH). Anal. Calcd for C<sub>168</sub>H<sub>250</sub>N<sub>8</sub>O<sub>32</sub>·CHCl<sub>3</sub>: C, 67.36; H, 8.40; N, 3.72. Found: C, 67.18; H, 8.28; N, 3.74.**

**{4',5'-Bis(decoxy)benzo[1',2'-*k*]-1,4,7,10,13,16-hexaoxacyclooctadeca-2,11-dieno}[2,3-*e*]-1,3-diiminoisoindoline (**13**). Dicyanocrown ether **12** (720 mg, 1 mmol) and sodium methoxide (100 mg, 1.9 mmol) were placed in a three-necked flask equipped with a gas inlet and reflux condenser. The flask was flushed with anhydrous ammonia, and methanol (5 mL) and THF (5 mL) were added. The mixture was stirred at room temperature for 30 min and then refluxed for 4 h. During these periods, a stream of anhydrous ammonia was slowly bubbled through the solution. After cooling, chloroform was added, and the mixture was washed with water and centrifugated (3×). The solvent was removed under vacuum. Chloroform was again added, and the mixture was refluxed, cooled to room temperature, and finally filtered. The product was isolated after removal of the solvent under vacuum. Yield: 220 mg (30%). Light green solid. IR (CHCl<sub>3</sub>): 870 (Ar-H), 961 (Ar), 1015 (N-H), 1071, 1136 (C-O-C), 1285 (Ar-O-C), 1510, 1603 (Ar), 1658 (C=N), 2856, 2929 (CH<sub>2</sub>), 3275–3430 (N-H) cm<sup>-1</sup>. <sup>1</sup>H NMR (CDCl<sub>3</sub>, 100 MHz): δ 0.88 (t, 6H, CH<sub>3</sub>), 1.2–1.9 (m, 32H, CH<sub>2</sub>), 3.7–4.3 (m, 20H, CH<sub>2</sub>O), 6.57 (s, 2H, ArH), 7.2 (br s, ArH).**

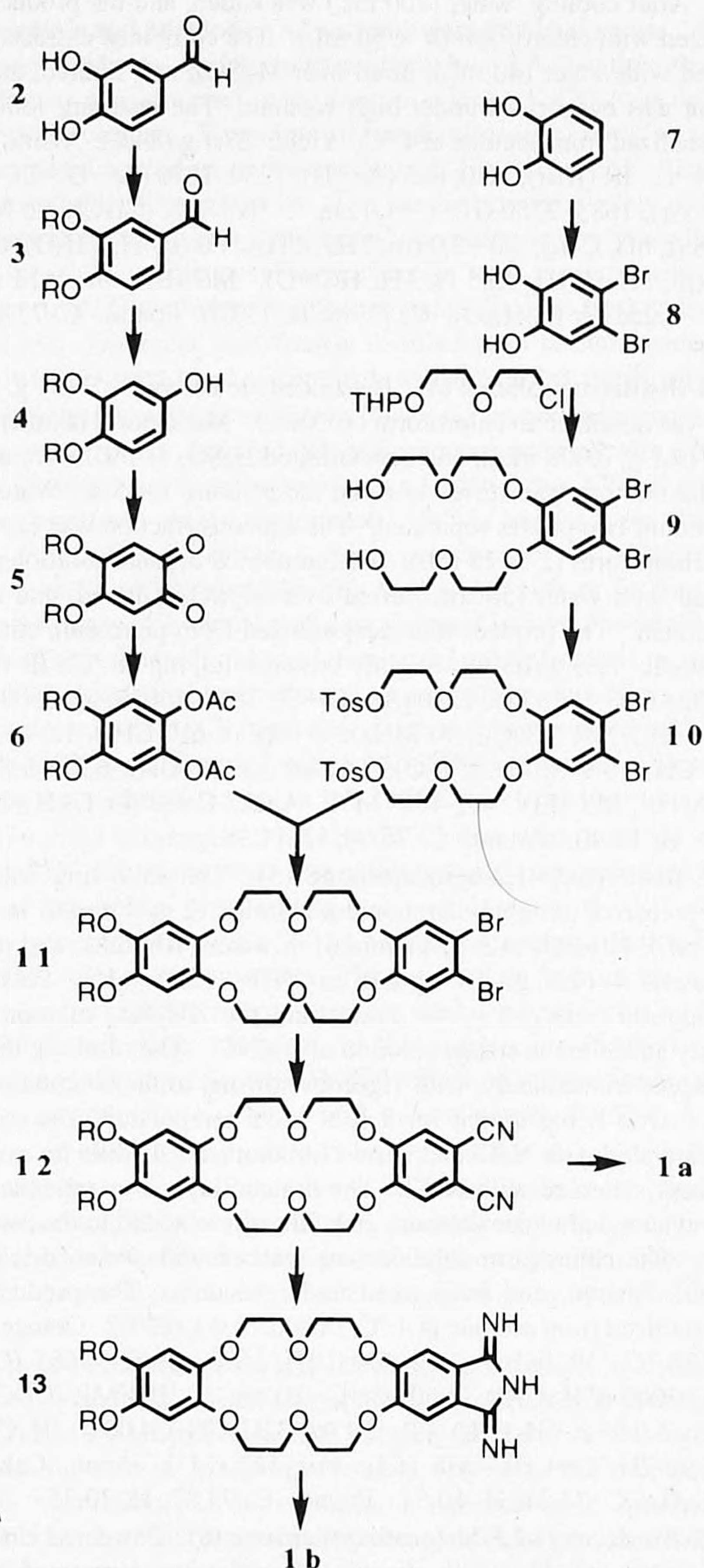
**(Tetrakis{4',5'-bis(decoxy)benzo[1',2'-*k*]-1,4,7,10,13,16-hexaoxacyclooctadeca-2,11-dieno}[2,3-*b*:2',3'-*i*:2'',3''-*p*:2''',3'''-*w*]phthalocyaninato)silicon Dihydroxide (**1b**). Diiminoisoindoline **13** (220 mg, 0.3 mmol) and quinoline (1 mL) were placed in a dry vessel. After the vessel was flushed with nitrogen gas, SiCl<sub>4</sub> (0.5 mL) was added, and the mixture was quickly brought to 190 °C and kept at this temperature for 1 h. Subsequently, the mixture was stirred for 16 h at 160 °C under a nitrogen atmosphere. After cooling, the resulting dichlorosilicon phthalocyanine was hydrolyzed by addition of water (10 mL), and the product was filtered off, washed with methanol and acetone, and subsequently extracted in a Soxhlet apparatus with methanol for 16 h to remove impurities. The product was obtained from the residue by Soxhlet extraction with chloroform and purified by chromatography (silica gel, chloroform–methanol 9:1 v/v). The first green fraction contained **1b**. The compound was recrystallized twice from chloroform by addition of acetone. Yield: 38 mg (17%). Dark green solid, decomp 178 °C. IR (CHCl<sub>3</sub>): 864 (Ar-H), 910, 948 (Pc), 1099 (Pc), 1135 (C-O-C), 1285 (Ar-O-C), 1509, 1607 (Ar/Pc), 2856, 2928 (CH<sub>2</sub>), 3500 (OH) cm<sup>-1</sup>. <sup>1</sup>H NMR (CDCl<sub>3</sub>, 100 MHz): δ 0.87 (t, 24H, CH<sub>3</sub>), 1.1–2.0 (m, 128H, CH<sub>2</sub>), 3.8–4.9 (m, 80H, CH<sub>2</sub>O), 6.65 (s, 8H, ArH), 8.93 (s, 8H, PcH). Anal. Calcd for C<sub>168</sub>H<sub>250</sub>N<sub>8</sub>O<sub>34</sub>Si: C, 68.31; H, 8.53; N, 3.79. Found: C, 67.76; H, 8.50; N, 3.69.**

## Results and Discussion

**Synthesis and Characterization.** The synthesis of phthalocyanine **1a** has been described in a preliminary communication<sup>10</sup> and is summarized in Scheme 1. Synthetic details are given in the Experimental Section.

Surprisingly, the solubility of **1a** in organic solvents was extremely low. At room temperature, the compound was found to be slightly soluble in chloroform and toluene only. The solubility in these solvents could be improved with heating. The <sup>1</sup>H NMR spectrum of **1a** in CDCl<sub>3</sub> displayed broad signals, and the protons of the Pc core were invisible, even at elevated temperatures. As will be shown in the next section, this effect is due to strong aggregation of the molecules. Although the product had been dried extensively in high vacuum for several

## Scheme 1



days, elemental analysis revealed that some chloroform was retained in the solid (molar ratio CHCl<sub>3</sub>/**1a** ≈ 1).

The dihydroxysilicon derivative **1b** was synthesized in two steps from dicyanide **12** (Scheme 1). The latter compound was first converted into the 1,3-diiminoisoindoline **13** by reaction with ammonia in 1:1 (v/v) THF–methanol (yield 30%). Subsequent cyclization of **13** in quinoline in the presence of SiCl<sub>4</sub>, followed by hydrolysis of the resulting dichlorosilicon Pc, gave **1b** in 17% yield. In contrast to the metal-free derivative **1a**, compound **1b** was found to be highly soluble in chloroform. A nicely resolved <sup>1</sup>H NMR spectrum could be recorded, including the peaks of the Pc protons. This result suggests that aggregation of **1b** is prevented by the axial hydroxy substituents. The UV/vis spectrum of **1b** displayed a strong Q-band at 679 nm (see Figure 2), which is in line with values found for other dihydroxysilicon Pcs.<sup>8c,14</sup>

We polymerized phthalocyanine **1b** using two different methods, *viz.* as described by van der Pol *et al.*<sup>14</sup> and by Caseri *et al.*<sup>15</sup> The first method afforded a purple insoluble polymer, whereas the second method resulted in a blue pentamer. The

(14) van der Pol, J. F.; Zwicker, J. W.; Warman, J. M.; de Haas, M. P. *Recl. Trav. Chim. Pays-Bas* **1990**, *109*, 208–215.

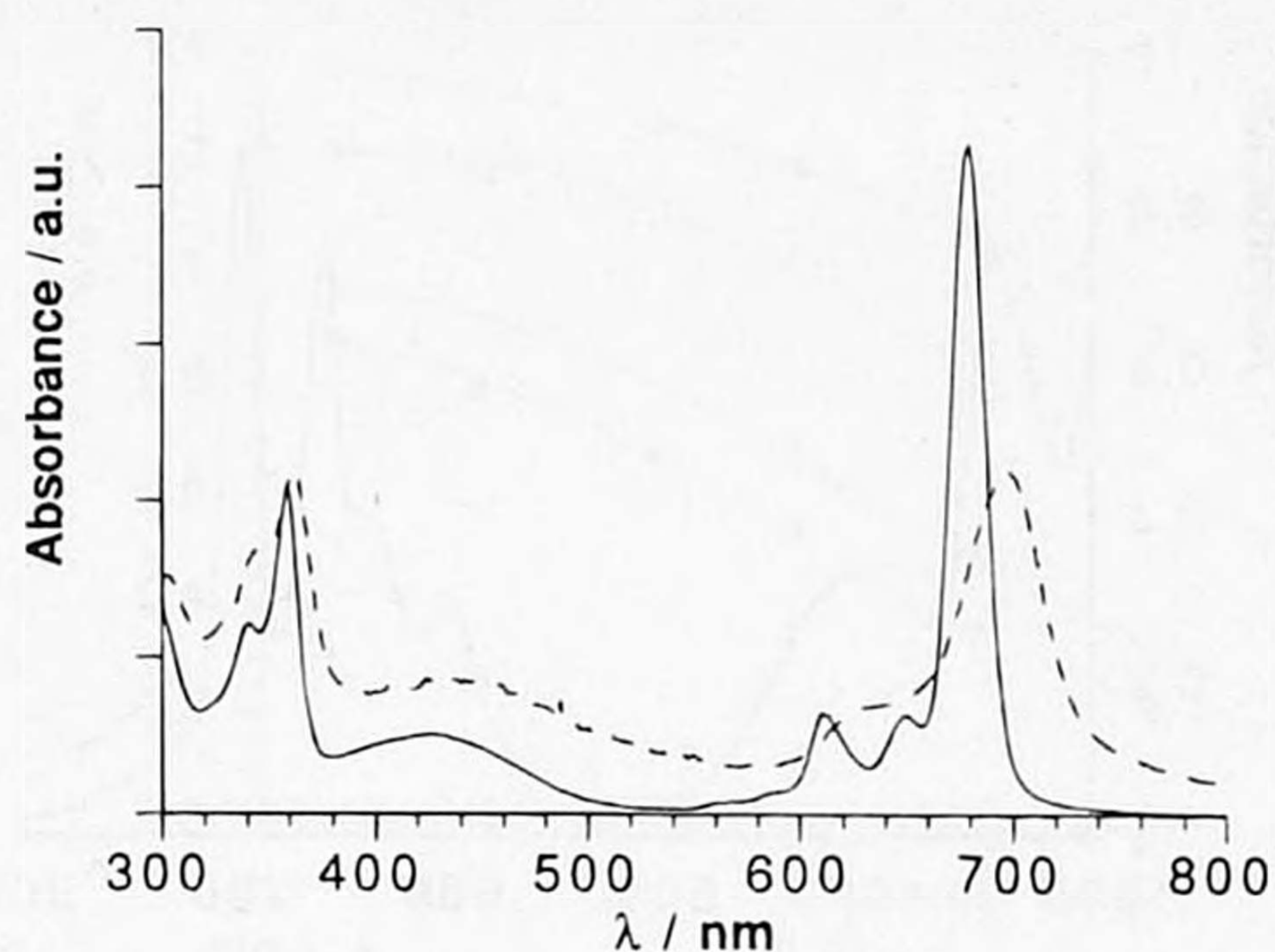


**Figure 2.** Electronic absorption spectra of **1b** in chloroform solution (—), and in a  $2 \times 10$ -layer LB film (---).

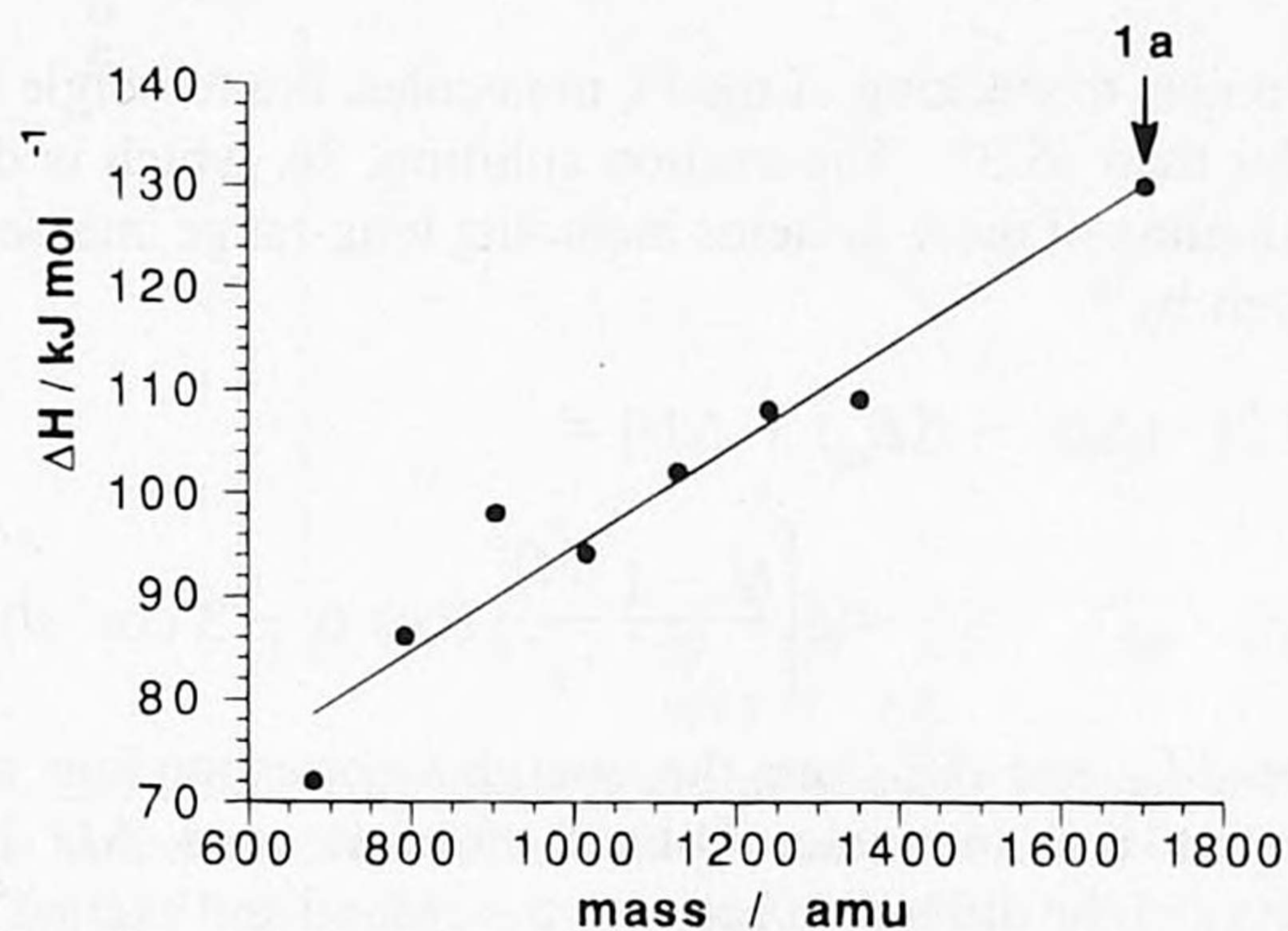


**Figure 3.** Transition enthalpy *versus* the total mass of the side chains of octa(alkoxy)-Pcs (6–12 carbon atoms per chain, data taken from ref 7d) and of **1a**. Only the flexible parts of the substituents are included in the calculation of the total mass (see text).

degree of polymerization of the latter oligomer was determined by comparing the exciton shift of the Q-band with the Q-band of the monomer. Details about the polymerization of **1b** and the properties of the polymer will be presented in a forthcoming paper.

**Solid State and Mesophase Structures.** The phase behavior of compound **1a** has been described previously.<sup>10</sup> One reversible transition from the solid to the mesophase was detected by DSC, with the peak onset in the heating run found at 148 °C (cooling run, 105 °C). The transition enthalpy amounted to 130  $\text{kJ}\cdot\text{mol}^{-1}$ . This value is  $\sim 20 \text{ kJ}\cdot\text{mol}^{-1}$  larger than the value reported for the crystalline phase to mesophase transition of octa(dodecoxy)phthalocyanine.<sup>5d</sup> This is due to the fact that the substituents of **1a** are larger than those of the aforementioned phthalocyanine. Figure 3 shows a plot of the transition enthalpies of octa(alkoxy)phthalocyanines, together with that of **1a**, *versus* the total molar mass of the flexible parts of the substituents. For the calculation of this molar mass, the rigid benzene rings of **1a**, as well as the oxygen atoms connected to these benzene rings and those connected to the Pc cores of **1a** and the other octa(alkoxy)-Pcs, were excluded. The following linear relationship was found:  $\Delta H = 44.4 + 0.05m_{\text{flex}}$ , with  $m_{\text{flex}}$  being the total flexible mass of the substituents in atomic mass units. At the crystalline phase to mesophase transition, the side chains of the octa(alkoxy)phthalocyanines start to melt.<sup>16</sup> The second term in the above equation, therefore, is likely to be equal to the melting enthalpy of these chains, which appears to be proportional to their mass. It can be concluded from Figure 3 that **1a** exhibits a melting behavior similar to that of the other liquid crystalline phthalocyanines.

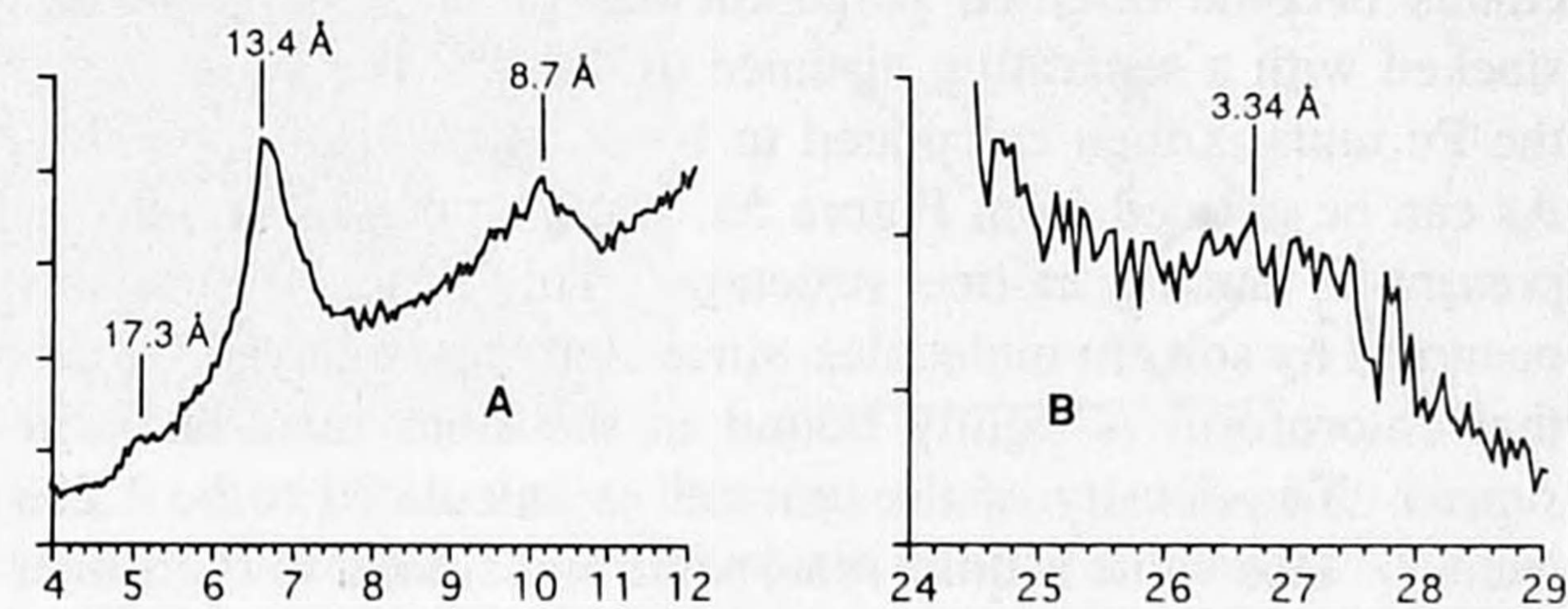
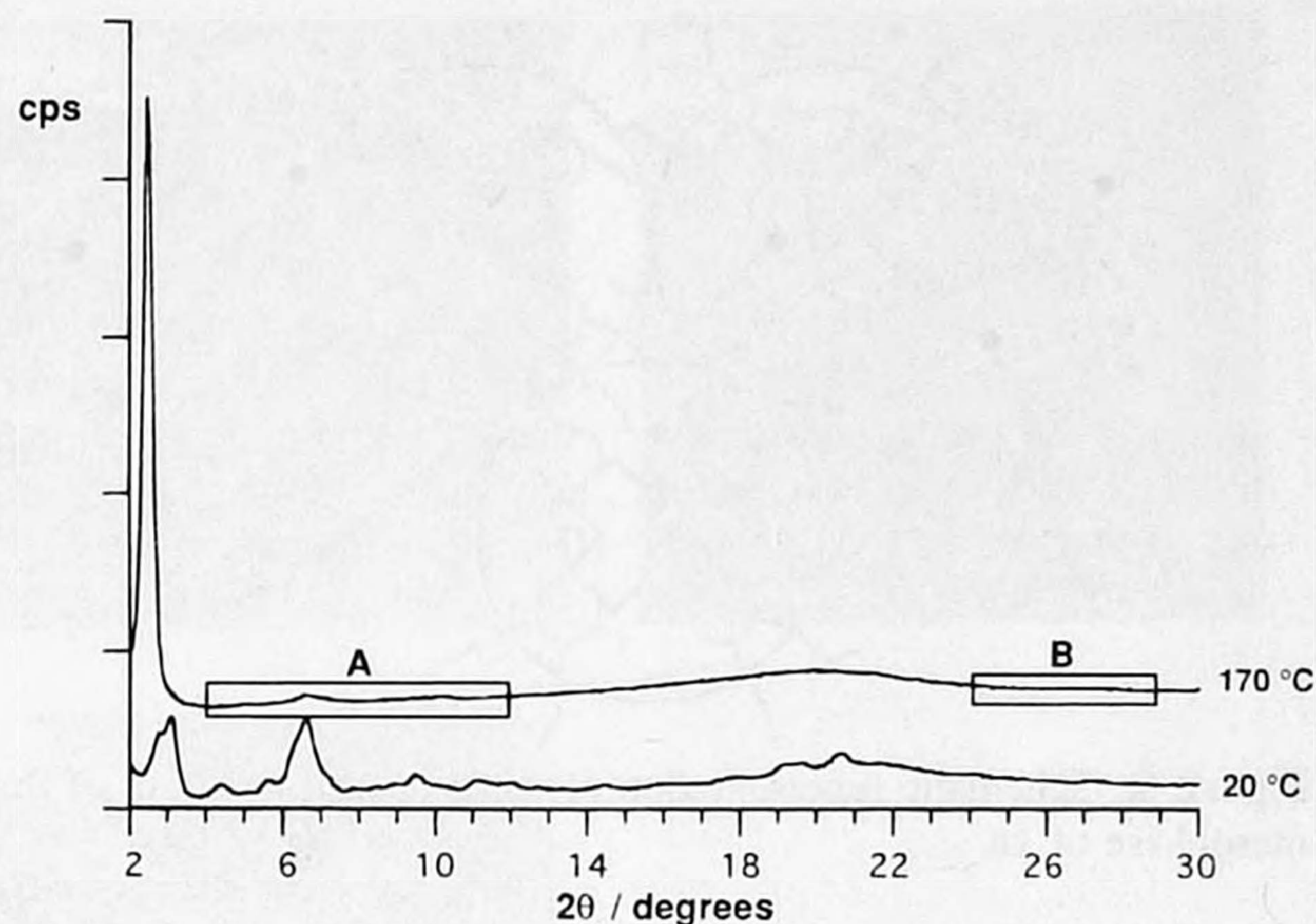


**Figure 4.** X-ray scattering curves of **1a** in the crystalline phase at 20 °C and in the mesophase at 170 °C. The curves are displaced along the y-axis to avoid overlapping.

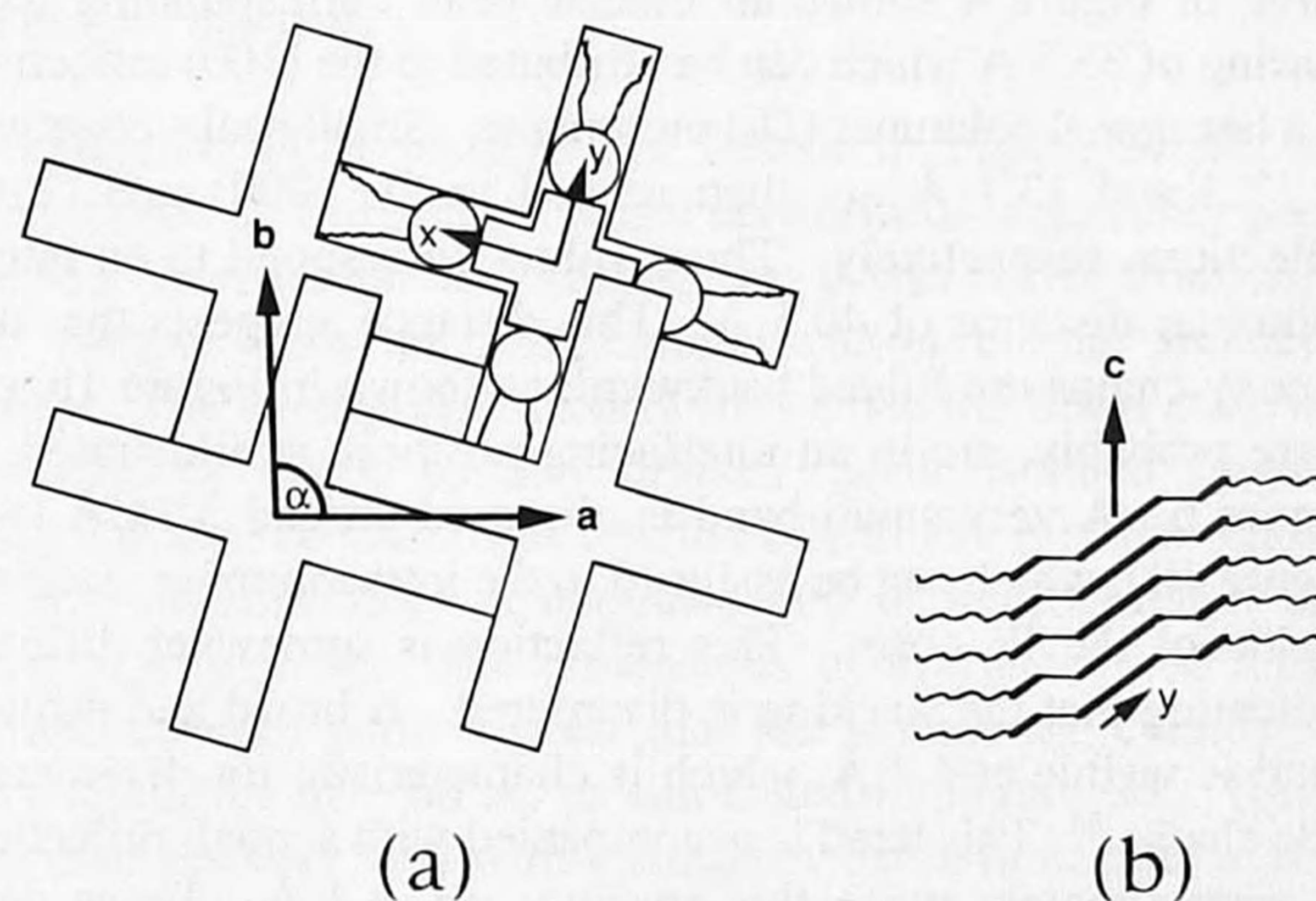


**Figure 5.** Schematic representation of the proposed structure of the crystalline phase of **1a**: (a) view along the normal on the Pc  $xy$ -plane and (b) view along the molecular  $x$ -axis.

DSC measurements on compound **1b** revealed no phase transition up to the temperature where the compound starts to polymerize, *i.e.*, at 178 °C.

The structures of the crystalline phase and the mesophase of **1a** were determined by SAXS measurements at 20 and 170 °C, respectively. The results are shown in Figure 4. The crystalline phase gives rise to a large number of peaks that can be indexed according to a monoclinic lattice with eclipsed Pc units having a unit cell with the parameters  $a = 31.2 \text{ \AA}$ ,  $b = 27.8 \text{ \AA}$ ,  $c = 4.3 \text{ \AA}$ , and  $\alpha = 96^\circ$ . With the help of molecular dimensions derived from CPK models, we propose a molecular arrangement as shown in Figure 5. The center-to-center distance of the Pc molecules along the  $a$ -axis is very close to the radius of a molecule with fully elongated decoxy chains, *i.e.*, 31.5 Å (see Figure 1a). The fact that the  $a$ - and  $b$ -axes are unequal indicates that the molecules are tilted. The Pc cores and the benzene rings are probably tilted with respect to the  $c$ -axis by rotations around the molecular  $x$ -axes, as illustrated in Figure 5b. This makes the inter-Pc distance very close to the van der Waals distance, *i.e.*, 3.4 Å, while the crown ether rings and the alkoxy

(15) Caseri, W.; Sauer, T.; Wegner, G. *Makromol. Chem. Rapid Commun.* **1988**, *9*, 651–657.

(16) Kentgens, A. P. M.; Markies, B. A.; van der Pol, J. F.; Nolte, R. J. *M. J. Am. Chem. Soc.* **1990**, *112*, 8800–8806.

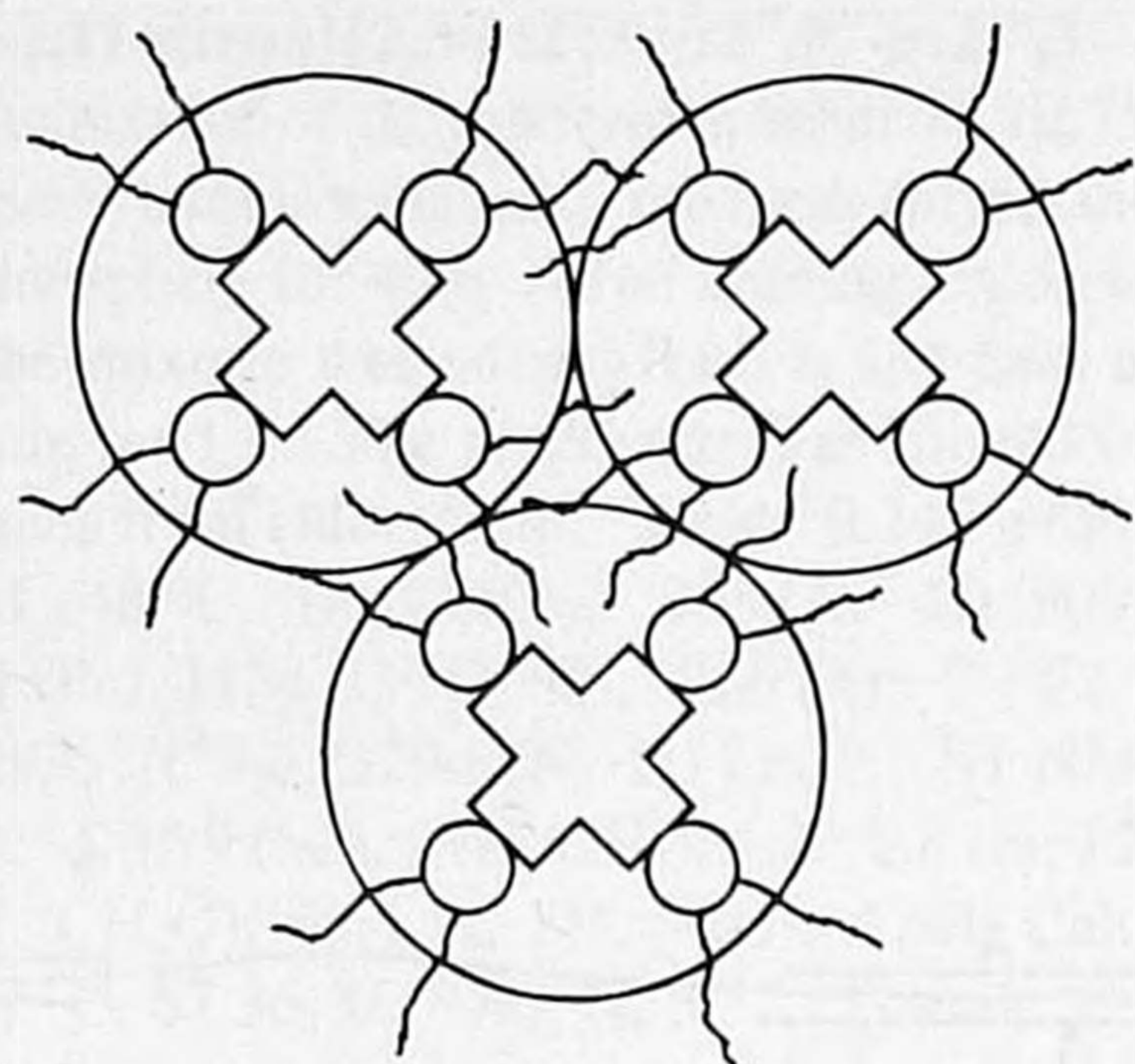


**Figure 6.** Schematic representation of the proposed structure of the mesophase of **1a**.

chains become oriented perpendicular to the *c*-axis and are stacked with a separating distance of 4.3 Å. The tilt angle of the Pc units is then calculated to be 38° ( $3.4/4.3 = \cos 38^\circ$ ). As can be noticed from Figure 5a, some empty space may be present in the crystalline structure. This space is probably occupied by solvent molecules, since elemental analysis reveals that chloroform is tightly bound in the solid material (*vide supra*). The density of the unit cell is calculated to be 1.293 g·cm<sup>-3</sup>. This value is quite reasonable and similar to the values found for other octa(alkoxy)-Pcs in the crystalline phase.<sup>5d</sup>

The SAXS measurements on **1a** at 170 °C confirmed the presence of a mesophase at this temperature. The scattering curve in Figure 4 shows an intense peak corresponding to a spacing of 35.3 Å which can be attributed to the (100) reflection of a hexagonal columnar (*D<sub>h</sub>*) mesophase. Small peaks observed at 17.3 and 13.4 Å are then related to the (200) and (210) reflections, respectively. These values correspond to an inter-columnar distance of 40.5 Å. This distance suggests that the decoxy chains are folded backward, as shown in Figure 1b, or, more probably, are in an interlacing position, as illustrated in Figure 6. A very small band is observed around 3.34 Å (see Figure 4B), which can be assigned to the intracolumnar stacking period of the Pc cores. This reflection is somewhat diffuse, indicating that the stacking is disordered. A broad and diffuse band is visible at 4.4 Å, which is characteristic for disordered side chains.<sup>5d</sup> This band is accompanied with a small reflection at approximately twice this spacing, *viz.* 8.7 Å. These data suggest that the Pc molecules are stacked cofacially in a staggered conformation. A density of 0.89 g·cm<sup>-3</sup> can be calculated for the unit cell of the mesophase of **1a**, which is very close to the density of metal-free octa(dodecoxy)-Pc in its mesophase.<sup>5d</sup>

An interesting feature of the structure of **1a** is the presence of ion channels: in the crystalline phase, the molecules are in an eclipsed position, with the crown ether rings superimposed. Also, in the mesophase, ion channels exist because the next-nearest crown ether rings are superimposed.

**Aggregation in Solution. (i) UV/Vis Spectroscopy.** The aggregation behavior of the metal-free phthalocyanine **1a** in chloroform solution was studied by UV/vis spectroscopy. Figure 7 shows the absorption spectra of a diluted solution (11 μM) of **1a** recorded at room temperature and at 50 °C. The high-temperature spectrum displays the split Q-band that is characteristic for nonaggregated metal-free Pcs, with maxima appearing at 661 and 700 nm. The spectrum recorded at room temperature is broadened, and the maximum is blue-shifted to 614 nm. According to the molecular exciton theory,<sup>17</sup> the blue

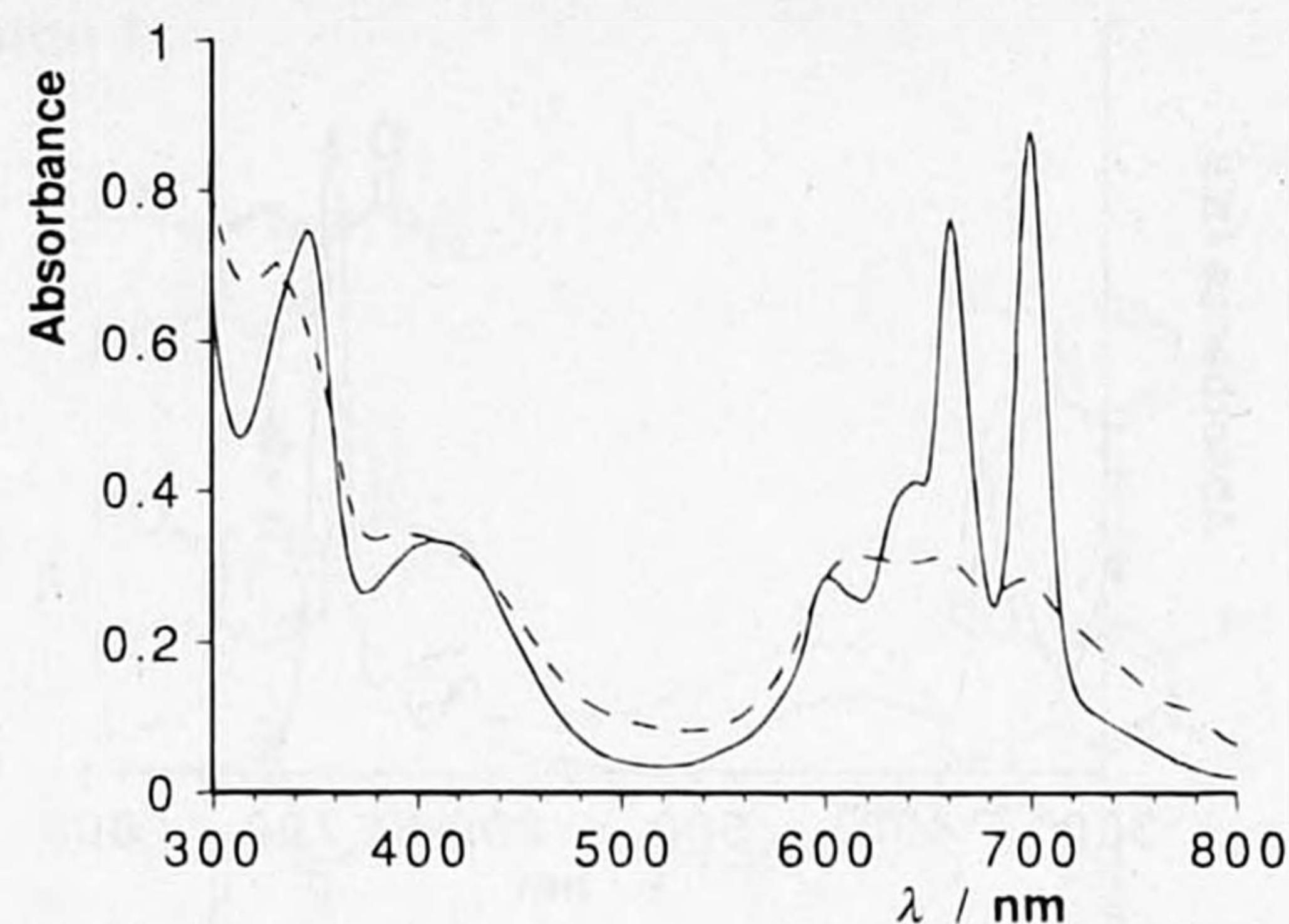


**Figure 7.** Electronic absorption spectra of **1a** in chloroform (11 μM) at different temperatures: (---) 25 and (—) 50 °C.

shift points to stacking of the Pc molecules, the tilt angle being smaller than 35.3°. The exciton splitting,  $2\epsilon$ , which is due to the coupling of the  $\pi$ -systems including long-range interactions, is given by<sup>18</sup>

$$2\epsilon = 2[-(\Delta E_a - \Delta E_m) + \Delta D] = -4.8 \left[ \frac{N-1}{N} \frac{|\bar{M}|^2}{r^3} (\cos \alpha - 3 \cos^2 \theta) \right] \quad (1)$$

where  $\Delta E_a$  and  $\Delta E_m$  are the energies corresponding to the aggregate and monomer Q-band maxima, and  $\Delta D$  is the lowering of the difference between the ground and excited states due to van der Waals interaction ( $\Delta D = -615 \text{ cm}^{-1}$ ).<sup>18</sup> The center-to-center distance between the molecules,  $r$ , is related to the angle  $\theta$  between the transition dipole moments ( $\bar{M}$ ) according to  $r = r_{\min}/\sin \theta$ , where the minimum van der Waals distance  $r_{\min} = 3.4 \text{ Å}$ .  $|\bar{M}|^2$  can be calculated from the oscillator strength  $f$ . The latter value was determined by integration of the monomeric Q-band, resulting in  $f = 0.59 \text{ erg}\cdot\text{cm}^{-1}$ , from which a value of  $|\bar{M}|^2 = 2.17 \times 10^{-19} \text{ cm}^2$  could be derived. These values are very close to the literature values found for a substituted dihydroxysilicon phthalocyanine.<sup>18</sup> When the aggregation number  $N$  is considered to be large, which is justified as shown in the next section, then  $(N-1)/N$  can be taken as unity by good approximation. With the values of  $\Delta E_a$  and  $\Delta E_m$  being 16 287 and 14 695  $\text{cm}^{-1}$ , respectively, and taking an eclipsed conformation (torsion angle  $\alpha = 0^\circ$ ), a value of  $\theta = 60^\circ$  was calculated using formula 1. This value corresponds to a tilt angle of 30° and a center-to-center distance  $r$  of 3.9 Å. If a staggered conformation is assumed ( $\alpha = 45^\circ$ ), then a tilt angle of 24° and  $r = 3.7 \text{ Å}$  are calculated. The latter structure cannot be ruled out, but the former is more plausible since the structural parameters are close to those of the  $\alpha$ -modification of solid unsubstituted Pcs.<sup>19</sup>

The aggregation of **1a** was found to be not only temperature dependent but also concentration dependent. The heat of association can be estimated from the temperature and concentration dependency of the UV/vis spectrum. Figure 8a shows a plot of the ratio of the absorbances of the aggregate and the monomer *versus* the temperature for four different concentrations of **1a** in chloroform. The aggregation number is related to this absorbance ratio: in other words, at a fixed ratio, the weight fraction of the monomer,  $m_1$ , is constant. For a constant  $m_1$ , the following relationship holds for linear aggregates of uniform structure:<sup>20</sup>

(18) Sauer, T.; Caseri, W.; Wegner, G. *Mol. Cryst. Liq. Cryst.* **1990**, *183*, 387–402.

(19) Wöhrle, D. *Kontakte (Darmstadt)* **1986**, *1*, 24–35.

(20) Ölschläger, H. *J. Colloid Interface Sci.* **1969**, *31*, 503–507.

(17) (a) Kasha, M.; Rawls, H. R.; Ashraf El-Bayoumi, M. *Pure Appl. Chem.* **1965**, *11*, 371–392. (b) Kasha, M. In *Spectroscopy of the Excited State*; DiBartolo, B., Ed.; Plenum Press: New York, 1976.

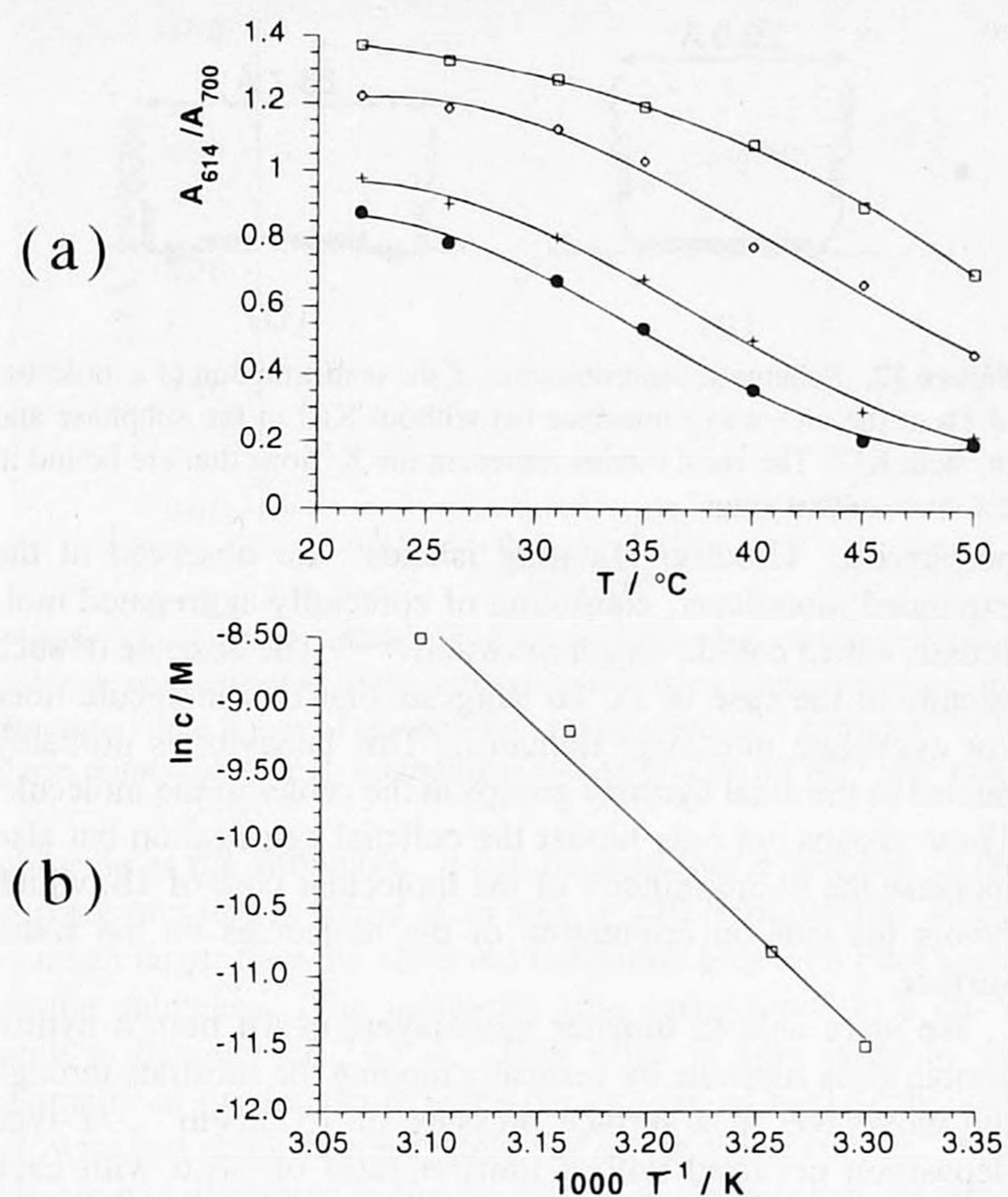


**Figure 8.** (a) Ratio of the absorbances at 614 and 700 nm plotted versus the temperature for various concentrations of **1a** in chloroform: 0.202 (□), 0.101 (◇), 0.020 (+), and 0.010 mM (●). (b) The temperatures  $T$  at which the absorbance ratio equals 0.7 were obtained by interpolation of the data points at each concentration  $c$  and plotted (b) as  $\ln c$  versus  $1/T$ .

$$W_1 = R \frac{\Delta \ln c}{\Delta(1/T)} \quad (2)$$

where  $W_1$  is the heat of association,  $R$  is the gas constant,  $\Delta \ln c$  is the difference between two Pc concentrations, and  $\Delta(1/T)$  is related to the temperature difference that has to be applied to maintain a constant  $m_1$ . The values of  $T$  where the absorbance ratio has a constant but arbitrary chosen value (0.7 in this case) were obtained by interpolation of the data points of Figure 8a at each concentration. The plot of  $\ln c$  versus the reciprocal temperature (Figure 8b) afforded a straight line, from which a value of  $W_1 = -125 \text{ kJ}\cdot\text{mol}^{-1}$  was derived. To our knowledge, such a high value has never before been reported in the literature for the aggregation of Pcs. For example, the heats of association of tetrasulfonatophthalocyanines in water are 2.5–5 times lower.<sup>21</sup> The driving forces for aggregation in this literature example are  $\pi$ – $\pi$  interactions, van der Waals interactions, and, in particular, hydrophobic effects. The aggregation of Pc **1a** in chloroform is mainly the result of  $\pi$ – $\pi$  and van der Waals interactions. These interactions are exceptionally strong in our system because they can take place not only between the Pc cores but also between the peripheral benzene units of different eclipsed molecules, resulting in a five-points attachment. The existence of strong attraction between the molecules of **1a** leads to extremely long linear aggregates, as will be shown next.

**(ii) Electron Microscopy.** Interestingly, when a more concentrated solution of compound **1a** in hot chloroform was cooled to room temperature, a firm gel was formed. This was observed at concentrations as low as  $7 \text{ mg}\cdot\text{mL}^{-1}$ . A sample having the latter concentration and a sample of  $1 \text{ mg}\cdot\text{mL}^{-1}$  were studied with transmission electron microscopy (TEM). Some

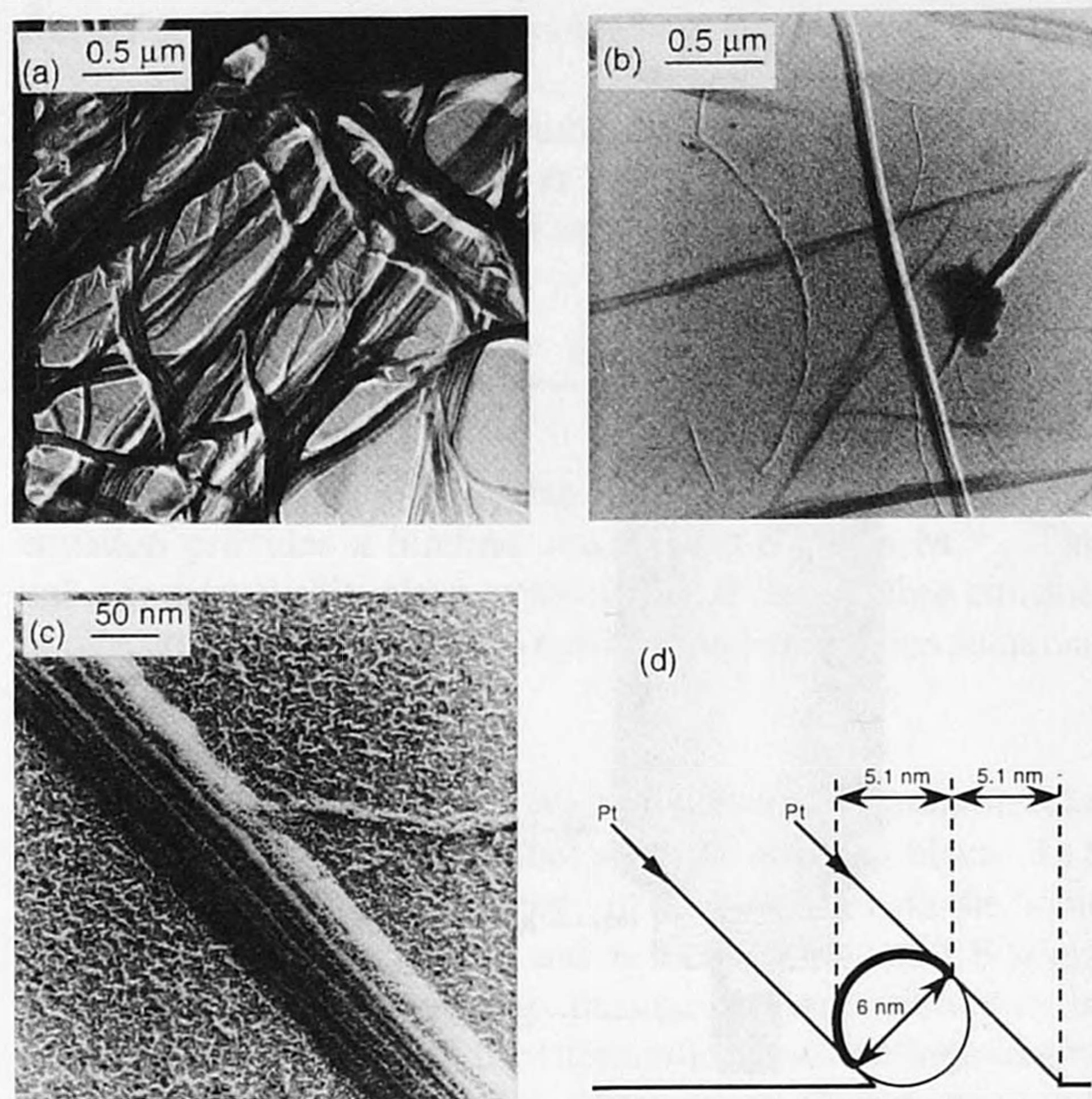


**Figure 9.** (a–c) Transmission electron micrographs of a gel of **1a** in chloroform ( $7 \text{ mg}\cdot\text{mL}^{-1}$ ). (d) Schematic illustration showing how a cylindrical structure of 60 Å diameter is covered when shadowed with platinum vapor at an angle of 45°. When viewed from the top, this results in the appearance of a covered and an uncovered parallel stroke of 51 Å width each, corresponding with the dimensions observed in the TEM micrographs.

representative TEM pictures are shown in Figure 9. At a concentration of  $7 \text{ mg}\cdot\text{mL}^{-1}$ , dense networks of large fibers are observed (micrograph a). Micrograph b was taken from the same sample with the same magnification but at another position. The latter picture clearly shows that the fibers consist of bundles of single parallel strands. Some isolated single strands can also be seen. The length of the fibers is of the order of a few micrometers. A magnification of micrograph b is shown in Figure 9c. The dimensions of the uncovered and platinum-covered parts suggest that the strands are cylinders with a diameter of  $\sim 60 \text{ \AA}$ , as illustrated in Figure 9d. This value matches very well with the diameter of a molecule of **1a** as estimated from CPK molecular models (see Figure 1a). At the lower concentration of  $1 \text{ mg}\cdot\text{mL}^{-1}$ , fibers are also observed, but they are smaller in length and no network is formed (not shown).

From these results, we may conclude that compound **1a** self-assembles in chloroform solution to produce linear aggregates. The stacks that are visualized by TEM have molecular thickness and are built up from  $\sim 10^4$  molecules. Such a large aggregation number in solution is unprecedented and reflects the existence of large attracting forces between the molecules. As discussed in the UV/Vis Spectroscopy section, the molecules are most likely stacked in an eclipsed conformation. Such a conformation was also shown to be present in the crystalline state of **1a**. A (close to) eclipsed conformation places the peripheral benzene units in a favorable position for  $\pi$ – $\pi$  interaction. This has interesting consequences. The isolated strands of molecules **1a** can be considered as being molecular cables (Figure 10). Such cables contain a central electron-conducting wire of stacked Pc molecules, four ion channels formed by the crown ether rings, and a surrounding insulating hydrocarbon mantle. The electron- and ion-conducting properties of the solid and the mesophase, as well as of the aggregates in solution, will be the subject of future studies.

**Formation of Monolayers and LB Films.** It was not

(21) (a) Kratky, O.; Ölschläger, H. *J. Colloid Interface Sci.* **1969**, *31*, 490–502. (b) Farina, R. D.; Halko, D. J.; Swinehart, J. H. *J. Phys. Chem.* **1972**, *76*, 2343–2348.



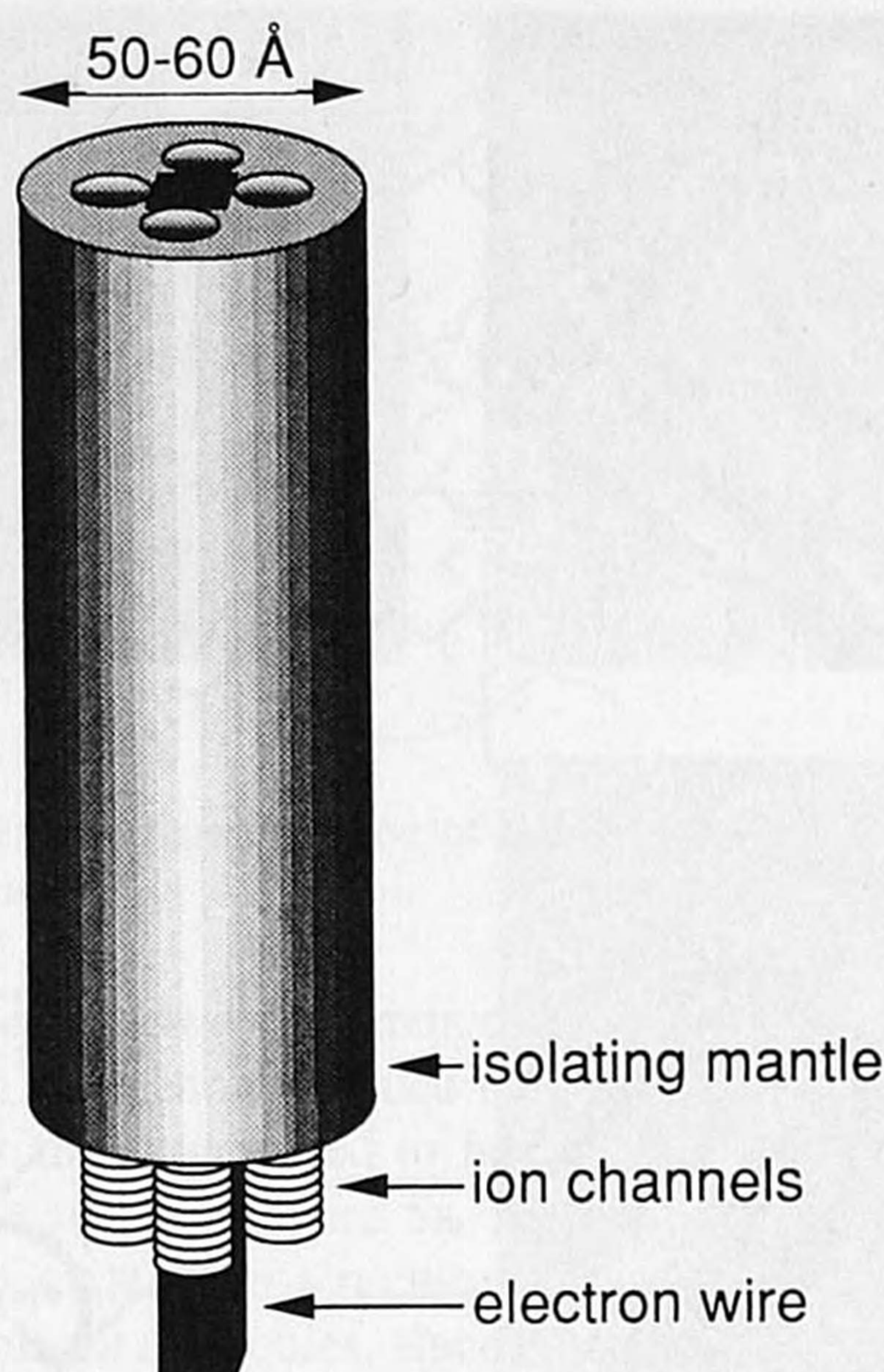


**Figure 10.** Schematic representation of the multiwired molecular cable formed by aggregation of **1a** in chloroform.

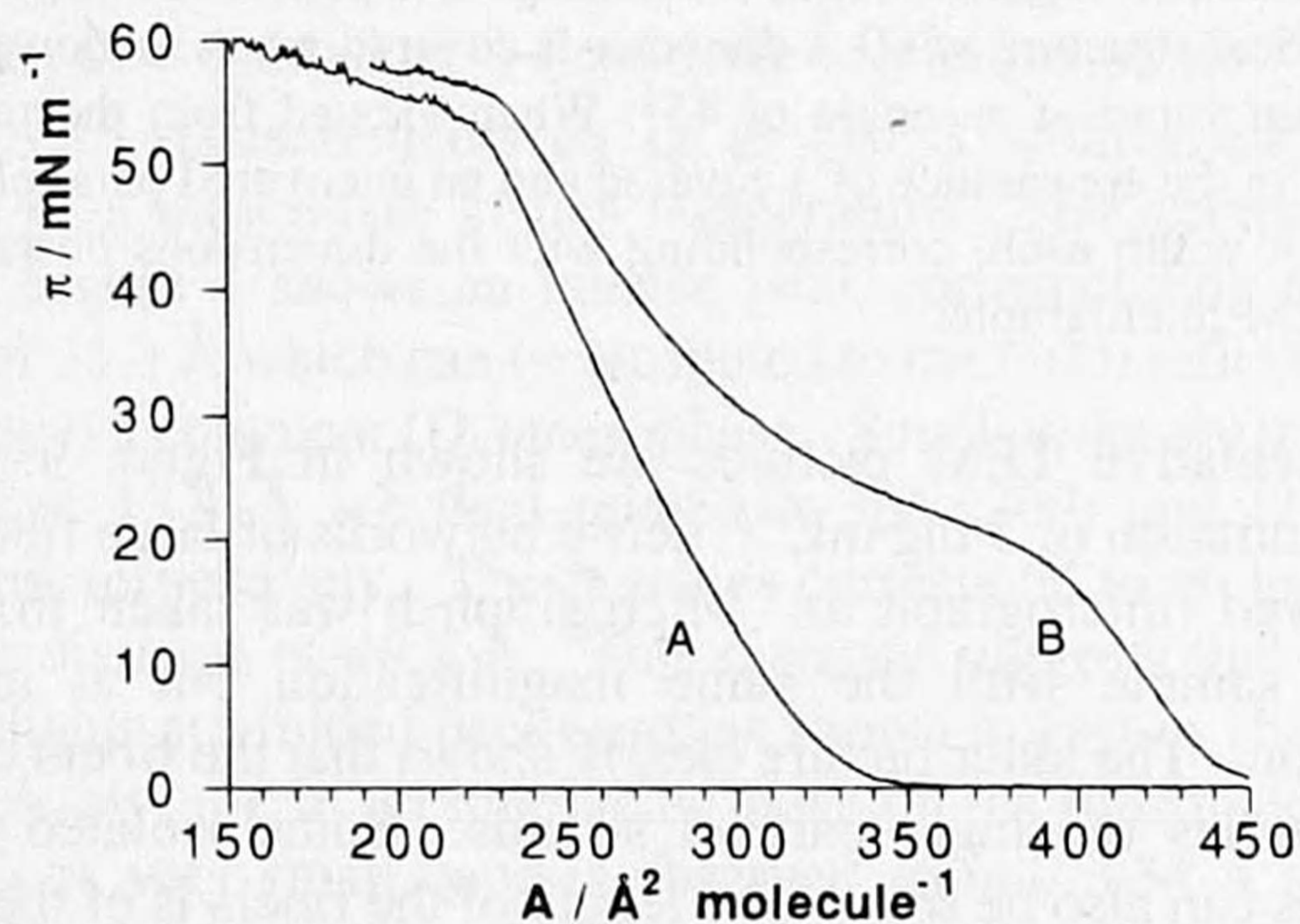


**Figure 11.** Surface pressure–surface area isotherms for **1b** at a subphase temperature of 20 °C. Curve A, pure water; curve B, 1 M KCl.

possible to form monomolecular layers from **1a** at the air–water interface due to the strong tendency of the molecules to aggregate. The dihydroxysilicon derivative **1b** does not aggregate in organic solution. This compound turned out to be suitable for the formation of LB films, as will be shown next.

A solution of **1b** in chloroform was spread on a water surface at 20 °C. Figure 11, curve A, shows the surface pressure–surface area ( $\pi$ – $A$ ) isotherm. A continuous rise of the pressure with decreasing area was observed up to  $\pi = 53 \text{ mN}\cdot\text{m}^{-1}$ , whereupon the film collapsed. Extrapolation of the steepest part of the curve to zero pressure gave a very large area of  $313 \text{ \AA}^2/\text{molecule}$ . This value is too high for an edge-on arrangement of the molecules on the water surface. A side-on orientation of the Pc core with the substituents oriented away from the water surface fits well with the measured area per molecule. Assuming a circular projection of the molecule on the water surface, a diameter of  $20.0 \text{ \AA}$  can be derived from the measured area per molecule, which is in agreement with the dimensions of CPK molecular models of such a conformation (see Figure 12a).

During the recording of the pressure–area isotherm, we viewed the water surface with a Brewster angle microscope (BAM). Both the expanded ( $\pi = 0$ ) and the compressed monolayers ( $\pi > 0$ ) displayed a completely structureless surface. Only when the collapse pressure was reached did lines appear due to the formation of multilayers. This behavior is in striking contrast with that of many other monolayer-forming Pcs and

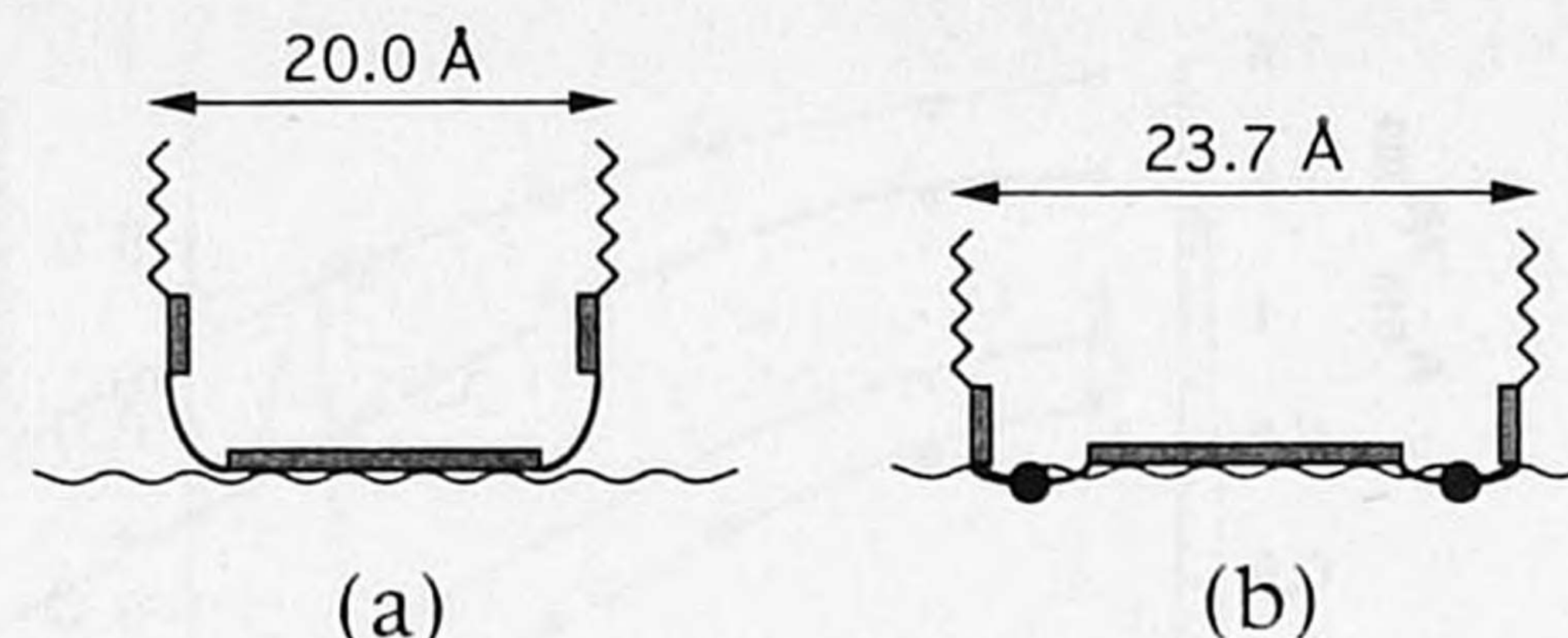


**Figure 12.** Schematic representation of the conformation of a molecule of **1b** at the air–water interface (a) without KCl in the subphase and (b) with KCl. The solid circles represent the  $\text{K}^+$  ions that are bound in the crown ether rings.

porphyrins. Usually, “floating islands” are observed at the expanded monolayer, consisting of cofacially aggregated molecules, which collide on compression.<sup>6h,22</sup> The absence of such islands in the case of Pc **1b** suggests that this molecule does not aggregate into large domains. This behavior is probably related to the axial hydroxy groups in the center of the molecule. These groups not only hinder the cofacial aggregation but also increase the hydrophilicity of the molecular core of **1b**, which favors the side-on orientation of the molecules on the water surface.

We were able to transfer monolayers of **1b** onto a hydrophobic glass substrate by vertically dipping the substrate through the monolayer at a surface pressure of  $15 \text{ mN}\cdot\text{m}^{-1}$ . Y-type deposition occurred with a transfer ratio of  $\sim 1.0$  with each upstroke transfer. The downstroke transfer resulted in a lower ratio of  $\sim 0.5$ , which might be the result of an incomplete transfer or a conformational change of the molecules during the deposition process. The UV/vis spectrum of a  $2 \times 10$ -layer film is shown in Figure 2. The maximum of the Q-band is seen at  $697 \text{ nm}$ , which is red-shifted compared to the Q-band of a chloroform solution of **1b** (*vide infra*). An additional small peak is observed at  $630 \text{ nm}$ . These spectral changes can be attributed to exciton splitting due to a slipped cofacial stacking of the Pc units with a tilt angle larger than  $35.3 \text{ \AA}$ . The smaller peak is the result of a transition that is only weakly allowed by the selection rules when the intermolecular torsion angle  $\alpha$  is larger than zero.<sup>17</sup> Similar spectral changes were observed in solid films of axially substituted silicon naphthalocyanines.<sup>23</sup> The observed energy difference between the allowed and partly forbidden transition,  $2\epsilon$ , amounts to  $1526 \text{ cm}^{-1}$ . We can calculate the aggregation number  $N$  from this exciton splitting with the help of formula (1), taking for the center-to-center distance  $r$  the value that was previously measured for the dihydroxysilicon derivative of octa(alkoxy)-Pc, *i.e.*,  $4.5 \text{ \AA}$ .<sup>24</sup> This value corresponds to  $\theta = 49.1^\circ$  or a tilt angle of  $40.9^\circ$ . The numerical factor in formula 1 has to be reduced to 4.0 to exclude longer range interactions. If we take for the torsion angle between the molecules the value  $\alpha = 0^\circ$ , the upper limit of  $N$  can be calculated; for  $\alpha = 45^\circ$ , the lower limit is found. These limits amount to 2.3 and 1.4, respectively. From these numbers, we may conclude that the molecules in the LB film are present as dimers. This result is in line with the observed Y-type deposition, which results in an alternating “face-to-face” and “tail-to-tail” multilayer structure.

**Binding of Cations in Monolayers.** Figure 11, curve B, shows the isotherm that was recorded with 1 M potassium

(22) See, for example: (a) Kroon, J. M.; Sudhölter, E. J. R.; Schenning, A. P. H. J.; Nolte, R. J. M., *Langmuir* **1995**, *11*, 214–220. (b) Gelinck, G. H.; van Nostrum, C. F., unpublished results. For phthalocyanines that do not display this behavior, see: (c) Burghard, M.; Schmelzer, M.; Roth, S.; Haisch, P.; Hanack, M. *Langmuir* **1994**, *10*, 4265–4269. (d) Hua, Y. L.; Roberts, G. G.; Ahmad, M. M.; Petty, M. C.; Hanack, M.; Rein, M. *Philos. Mag.* **1986**, *B53*, 105–113.

(23) Katayose, M.; Tai, S.; Kamijima, K.; Hagiwara, H.; Hayashi, N. *J. Chem. Soc., Perkin Trans. 2* **1992**, 403–409.

(24) Sauer, T.; Wegner, G. *Mol. Cryst. Liq. Cryst.* **1988**, *162B*, 97–118.

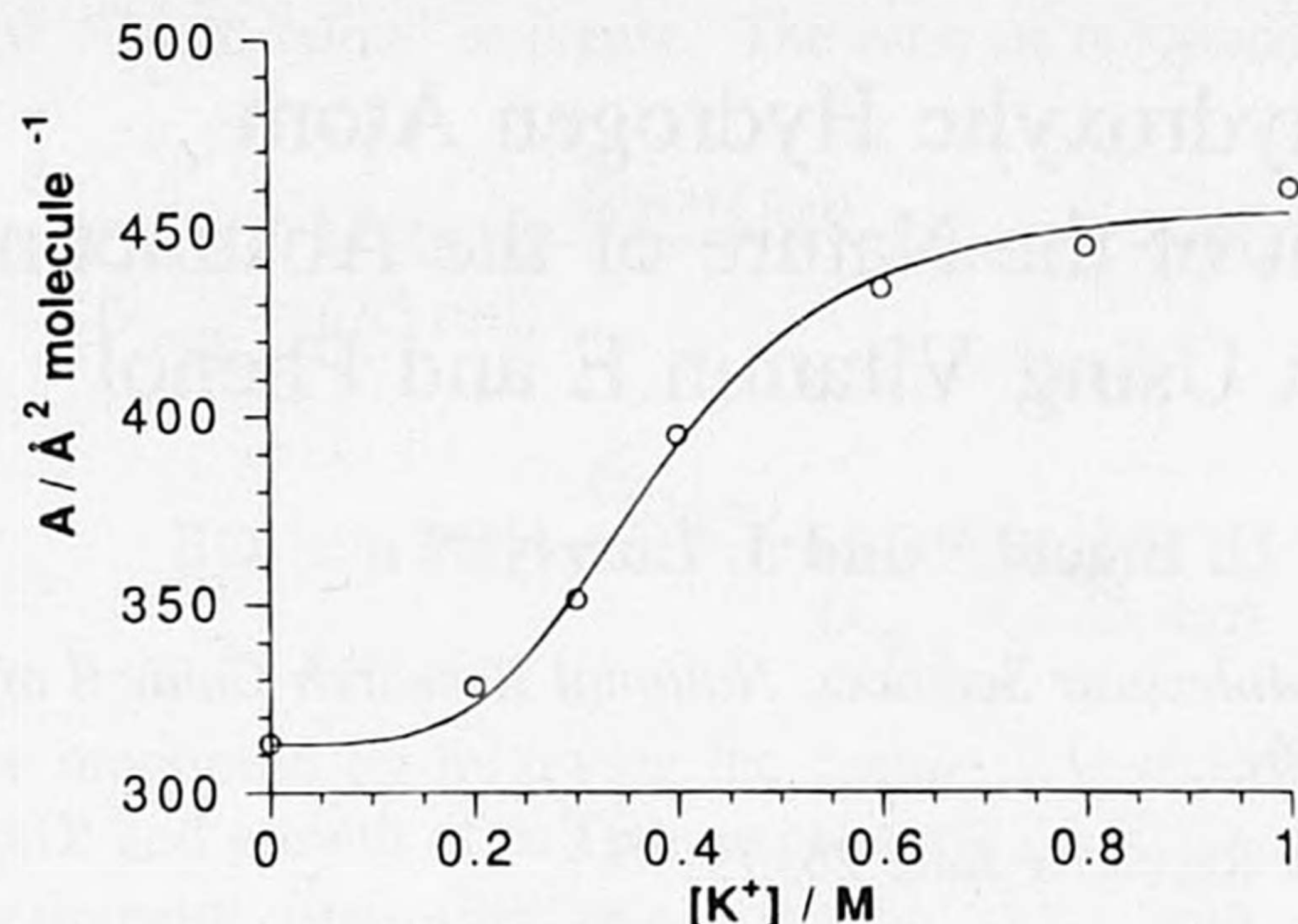
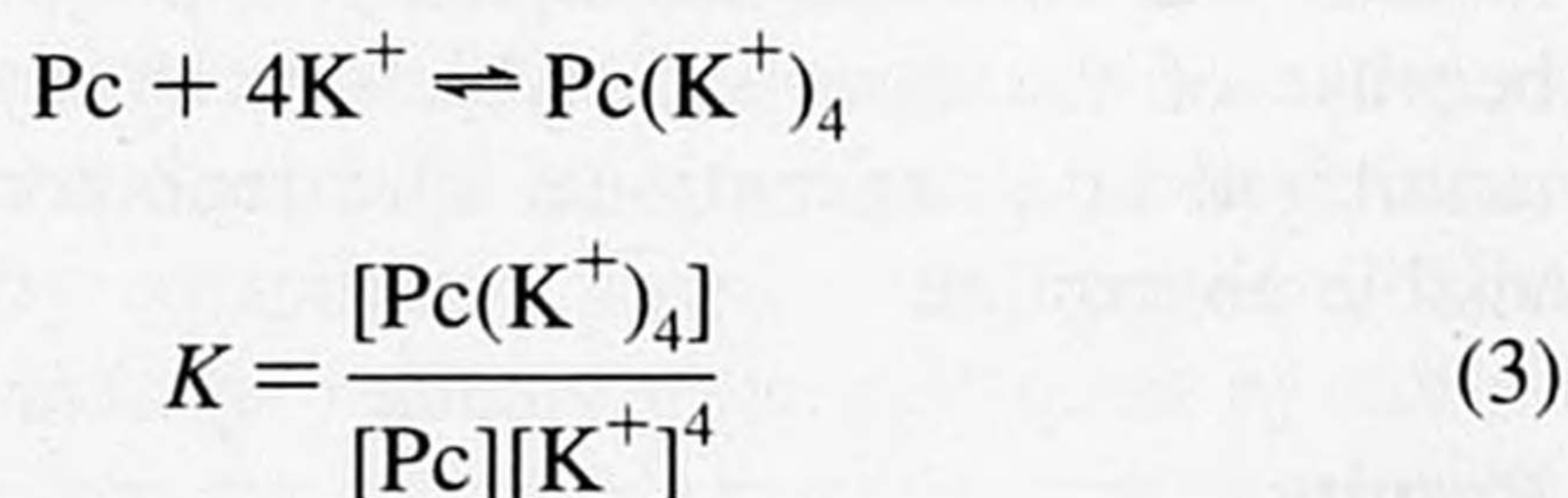


**Figure 13.** Area per molecule of **1b** as a function of the potassium chloride concentration in the subphase. The open circles represent the measured data points. The solid line is the result of a computer fit of these points, leading to a binding constant of  $K = 48 \text{ M}^{-1}$  (see text).

chloride as the subphase. It can be seen that a first rise of the surface pressure is found at an area of  $440 \text{ Å}^2/\text{molecule}$ , which is much larger than the observed molecular area with pure water as the subphase. The increased area corresponds to a circle with a diameter of  $23.7 \text{ Å}$ . This value is very close to the diameter of the molecule when the Pc core as well as the four crown ether rings lie completely flat on the water surface. This situation is illustrated in Figure 12b. It is obvious that the alkali metal ions induce a conformational change of the molecules of **1b** at the air–water interface. The binding of the metal ions in the crown ether rings make these macrocycles more rigid and more hydrophilic, favoring their interaction with water. Figure 11 shows that a phase transition takes place when the monolayer area of **1b** on 1 M KCl is decreased. A second rise of the surface pressure is found at an area that is close to the molecular area on pure water. Probably the decrease of the monolayer area forces the crown ether rings to lift from the water surface. It is not clear at present whether or not this results in the release of the cation.

We recorded isotherms at various subphase concentrations between 0 and 1 M KCl and measured the area per molecule related to the first surface pressure rise. Figure 13 shows a plot of the area per molecule versus the potassium ion concentration. We assume the following equilibrium and the corresponding binding constant  $K$ :



The concentrations of the complex and the free ligand can be calculated from the measured area per molecule,  $A$ , to be

$$[\text{Pc}(\text{K}^+)_4] = \frac{A - A_0}{A_c - A_0} [\text{Pc}]_0 \quad (4)$$

and

$$[\text{Pc}] = \frac{A_c - A}{A_c - A_0} [\text{Pc}]_0 \quad (5)$$

where  $A_0$  is the area per molecule on pure water,  $A_c$  is the area

per molecule when all complexation sites are occupied, and  $[\text{Pc}]_0$  is the total Pc concentration. By good approximation, the concentration of free potassium,  $[\text{K}^+]$ , is assumed not to be influenced by binding. This is true in our case because  $[\text{K}^+] \gg [\text{Pc}]_0$ . Combining eqs 3–5 results in the following relationship:

$$K = \frac{A - A_0}{A_c - A} [\text{K}^+]^{-4} \quad (6)$$

Computer fitting of the data points of Figure 13 to this equation provides a binding constant of  $K = 48 \text{ M}^{-1}$ . This value is remarkably close to the value of the binding constant of dibenzo-18-crown-6 with potassium ions in aqueous solutions, *viz.*  $46.5 \text{ M}^{-1}$ .<sup>25</sup>

### Concluding Remarks

We have described several ways to construct supramolecular structures from the novel phthalocyanine building blocks **1a,b** by a process of self-organization: in the solid state, in the liquid crystalline state, in solution, and as monolayers and LB films. Two features are assumed to be mainly responsible for the spontaneous formation of the supramolecules: the high degree of shape anisotropy of the Pcs, which favors their packing into columnar assemblies, and the fact that the molecules are strongly held together by van der Waals and  $\pi$ – $\pi$  interactions.

Very unexpected is the self-organization of **1a** in chloroform solution, leading to extremely long individual stacks of molecules. Aggregation of Pcs is usually observed in more polar solvents.<sup>8a</sup> The very high association energy which we determined from UV/vis spectroscopy experiments indicates that large attracting forces are responsible for this unique behavior. One-dimensional electron-conducting wires and ion-conducting channels are formed in the stacks, which are surrounded by an insulating hydrocarbon mantle.

The possibility to form monolayers and LB films from phthalocyanine **1b** is of interest for future applications. The ability of this compound to bind cations in its crown ether rings was demonstrated in monolayers. Interestingly, the obvious nonlinearity of the titration curve of Figure 13 is suggestive of a positive cooperative effect in the complexation of potassium ions, *i.e.*, a measurable change is observed only above a certain critical concentration of these ions. This result may be important for application in molecular switches based on the complexation of ions.<sup>26</sup>

**Acknowledgment.** We thank R. van Puijenbroek (AKZO Arnhem) for performing the SAXS measurements. The assistance of M. N. Teerenstra (University of Groningen) with the LB experiments, E. M. D. Keegstra (University of Utrecht) with the DSC and TGA measurements, and R. J. H. Hafkamp and H. P. M. Geurts (University of Nijmegen) with the EM experiments is gratefully acknowledged. This research was financially supported by the Dutch Innovation Oriented Research Programme (IOP) of the Ministry of Economic Affairs.

JA950698U

(25) Shchori, E.; Nae, N.; Jagur-Grodzinski, J. *J. Chem. Soc., Dalton Trans.* **1975**, 2381–2386.

(26) Toupance, T.; Ahsen, V.; Simon, J. *J. Am. Chem. Soc.* **1994**, *116*, 5352–5361.